Journal of Human Evolution 174 (2023) 103291

Contents lists available at ScienceDirect

Journal of Human Evolution

journal homepage: www.elsevier.com/locate/jhevol

# Reassessment of the human mandible from Banyoles (Girona, Spain)

Brian A. Keeling [a, *], Rolf Quam [a, b, c, d], Ignacio Martínez [d, e], Juan Luis Arsuaga [b, f], Julià Maroto [g]

[a] Department of Anthropology, Binghamton University, SUNY, New York, USA
[b] Centro UCM-ISCIII de Evolución y Comportamiento Humanos, Madrid, Spain
[c] Division of Anthropology, American Museum of Natural History, New York, USA
[d] Cátedra de Otoacústica Evolutiva y Paleoantropología (HM Hospitales-Universidad de Alcalá), Departamento de Ciencias de la Vida, Universidad de Alcalá, Madrid, Spain
[e] Centro de Investigación Francisco Javier Muñiz, Universidad de Buenos Aires, Calle Paraguay 2155, Primer piso, Ciudad Autónoma de Buenos Aires, 1121, Argentina
[f] Departamento de Geodinámica, Estratigrafía y Paleontología, Facultad de Ciencias Geológicas, Universidad Complutense de Madrid, Madrid, Spain
[g] Grup d'Arqueologia i Prehistòria, Universitat de Girona, pl. Ferrater Mora, 1, 17071 Girona, Spain

ARTICLE INFO

*Article history:*
Received 9 November 2021
Accepted 21 October 2022
Available online xxx

*Keywords:*
Pleistocene *Homo*
Human diversity
Modern human origins
3D geometric morphometrics
Mandibular morphology

ABSTRACT

Since the discovery of a human mandible in 1887 near the present-day city of Banyoles, northeastern Spain, researchers have generally emphasized its archaic features, including the lack of chin structures, and suggested affinities with the Neandertals or European Middle Pleistocene (Chibanian) specimens. Uranium-series and electron spin resonance dating suggest the mandible dates to the Late Pleistocene (Tarantian), approximately ca. 45–66 ka. In this study, we reassessed the taxonomic affinities of the Banyoles mandible by comparing it to samples of Middle Pleistocene fossils from Africa and Europe, Neandertals, Early and Upper Paleolithic modern humans, and recent modern humans. We evaluated the frequencies and expressions of morphological features and performed a three-dimensional geometric morphometric analysis on a virtual reconstruction of Banyoles to capture overall mandibular shape. Our results revealed no derived Neandertal morphological features in Banyoles. While a principal component analysis based on Euclidean distances from the first two principal components clearly grouped Banyoles with both fossil and recent *Homo sapiens* individuals, an analysis of the Procrustes residuals demonstrated that Banyoles did not fit into any of the comparative groups. The lack of Neandertal features in Banyoles is surprising considering its Late Pleistocene age. A consideration of the Middle Pleistocene fossil record in Europe and southwest Asia suggests that Banyoles is unlikely to represent a late-surviving Middle Pleistocene population. The lack of chin structures also complicates an assignment to *H. sapiens*, although early fossil *H. sapiens* do show somewhat variable development of the chin structures. Thus, Banyoles represents a non-Neandertal Late Pleistocene European individual and highlights the continuing signal of diversity in the hominin fossil record. The present situation makes Banyoles a prime candidate for ancient DNA or proteomic analyses, which may shed additional light on its taxonomic affinities.



## 1. Introduction

The human mandible from the site of Banyoles was accidentally discovered in 1887 during limestone quarrying operations near the town of Banyoles in northeastern Spain (Hernandez-Pacheco and Obermaier, 1915; Julià et al., 1987; Figs. 1 and 2). Historically, this mandible is one of the earliest fossil hominin discoveries on the Iberian Peninsula, and the specimen has a long history of study and analysis. Nevertheless, despite over a century of research, the taxonomic affinities of this fossil have remained elusive. Given the historical significance of the specimen, along with its fairly complete state of preservation and a clearer idea of its chronology, we undertook a reanalysis of the mandible from Banyoles (referred hereafter as Banyoles) relying on descriptive comparative morphology and quantitative three-dimensional geometric morphometrics (3D GM). We use these approaches to yield new insights into the taxonomic affinities of this mandible.

At the time of the mandible's discovery, the human fossil record consisted of only a few clearly recognizably nonmodern fossils, including the Neandertal child's skull from Engis in Belgium (1830;

* Corresponding author.
*E-mail address:* bkeelin1@binghamton.edu (B.A. Keeling).

https://doi.org/10.1016/j.jhevol.2022.103291
0047-2484/


**Figure 1.** Map of the Iberian Peninsula indicating the location where the Banyoles mandible was found (yellow star). Late Pleistocene Neandertal (orange triangles) and anatomically modern *Homo sapiens* (white squares with a blue outline) sites are shown for reference.

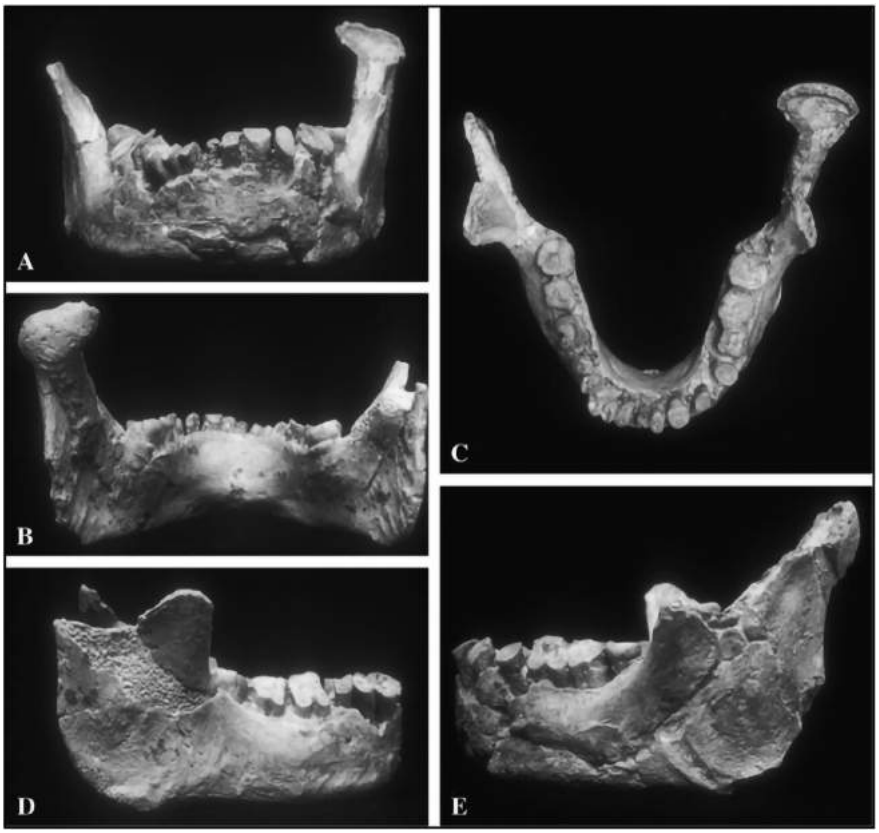


**Figure 2.** The Banyoles mandible in A) anterior, B) posterior, C) superior, D) right lateral, and E) left lateral views. Figure from Grün et al. (2006).

Schmerling, 1833–1834), the adult Neandertal cranium from Forbes' Quarry in Gibraltar (1848; Busk, 1865), the original Neandertal type specimen from Feldhofer Grotto (1856; Schaaffhausen, 1858), and the early *Homo sapiens* remains from Cro-Magnon (1868; Broca, 1868). Banyoles was found after Fraipont and Lohest (1887) demonstrated the antiquity of the Neandertal remains from Spy based on the presence of carbonaceous concretions on the bones similar to those found on extinct animal remains at this same site (Pirson et al., 2018). Thus, the discovery of Banyoles occurred at a time when the antiquity of human fossils was being increasingly

accepted, along with the notion that humans evolved from an ape-like ancestor.

Banyoles was encased in a limestone block when it was first discovered, and the travertine matrix was subsequently removed by Pere Alsius, a local pharmacist and naturalist, who exposed most of the external surface of the mandible and published two short descriptions of the fossil (Alsius, 1907, 1915). These were followed by the first monographic treatment of the specimen by Hernandez-Pacheco and Obermaier (1915) who aligned Banyoles with the Neandertals. Other authors of the time also generally emphasized resemblances to the Neandertals (MacCurdy, 1915; Sergi, 1917; Giuffrida-Ruggeri, 1921; Hoyos-Sáinz, 1947) or European Middle Pleistocene specimens (Bonarelli, 1916). In contrast, Keith (1931) noted a rudimentary expression of the chin present in Banyoles that is not typically seen in Neandertals. It was not until the 1950s that Santiago Alcobé (1993) undertook the task of extracting the mandible from the remaining adhering matrix and cleaning it. Thus, before 1956, all studies of Banyoles were done while it was still partially encased in the limestone travertine matrix, concealing the posterior and internal aspects of the mandible.

De Lumley (de Lumley, 1971–1972) provided the first detailed study of Banyoles after its restoration by Alcobé, noting some characteristics shared with European Middle Pleistocene (now Chibanian; Suganuma et al., 2021) mandibles, such as a relatively low corpus height, large condylar dimensions, and nontruncation of the gonial margin. De Lumley (de Lumley, 1971–1972) argued that the symphyseal region is most similar to Middle Pleistocene mandibles in lacking a mentum osseum, but with some features resembling recent *H. sapiens*, including a fairly vertical symphysis and a very shallow alveolar depression and slight lateral tubercles on the external surface.

A monograph on Banyoles and its context was published following an international conference in 1987 (Maroto, 1993). Contributions from numerous scholars characterized the mandible as a late Middle Pleistocene form of archaic genus *Homo* (de Lumley, 1993; Roth et al., 1993; Rosas, 1993). Sánchez-Lopez (1993) argued for a late Neandertal classification, but also noted some slight chin structures on the mandibular symphysis as potentially more modern-like features. Most recently, Alcázar de Velasco et al. (2011) also argued for the presence of some morphological features Banyoles shares with modern *H. sapiens*, including some chin structures. Nevertheless, studies that have included Banyoles in comparative samples generally consider it to represent either a Middle Pleistocene European (MPE) specimen or a Neandertal (Rosas, 2001; Mounier et al., 2009; Roksandic et al., 2011). Thus, despite the long history of research, scholars remain divided regarding the taxonomic affinities of this fossil. Part of this confusion seems to be linked to the lack of a clear archaeological context and date.

### 1.1. Context and dating of Banyoles

The town of Banyoles lies on a floodplain adjacent to Lake Banyoles, which has accumulated large amounts of limestone travertine since the Neogene (Hernandez-Pacheco and Obermaier, 1915; Julià et al., 1987; Maroto, 1987). The mandible was found east of Lake Banyoles in the Pla de la Formiga open quarry, which extends into the Pla de la Mata. Although the exact findspot cannot currently be located because of the continued quarrying activities at the site, the mandible was discovered around four meters below the surface in a limestone travertine tuff in the Pla de la Formiga quarry (Julià et al., 1987).

Faunal and floral remains were found near the mandible and can perhaps provide insights into the paleoenvironment of Banyoles, but no formal analysis of the faunal remains has been done (Julià et al., 1987). Nevertheless, the Pla de la Mata travertine matrix does contain Middle-Late Pleistocene species, including several species of *Equus* (horse), *Bos primigenius* (wild auroch), *Bison priscus* (steppe bison), and *Cervus elaphus* (red deer; Maroto and Soler, 1993).

Several isotopic studies have attempted to date the mandible. An early study by Berger and Libby (1966) radiocarbon dated the site to 17 ± 1.0 ka suggesting the mandible was much younger and postdated the Neandertals, in contrast to stratigraphic estimates of a Middle-Late Pleistocene age (Hernandez-Pacheco and Obermaier, 1915; Bonarelli, 1916; Solé Sabarís, 1957; Bech, 1971). Later, Yokoyama et al. (1987) performed a U-series analysis of a travertine sample of unknown provenience from the site as well as directly on the bone of the mandible itself. Yokoyama et al. (1987) modeled for both closed and open system behaviors and noted that the Banyoles bone was much younger (16.2 ± 3.2 ka) than the travertine for both a closed (ca. 70 ka) and open system (ca. 110 ka).

Shortly thereafter, Julià and Bischoff (1991) performed U-series analyses of a travertine sample which was removed from the mandible during Alcobé's restoration in 1956 as well as several travertine samples from different stratigraphic layers from the Pla de la Mata and the nearby Les Pedreres sediments. Their analyses yielded a date of 45 ± 4 ka for the travertine sample, suggesting this was the age of the fossil. The good agreement between the dates for the mandible and those from Pla de la Mata (45–50 ka) suggested the mandible most likely derived from this site, and the site likely represented a closed system, with no evidence of the mandible having been reworked (Julià and Bischoff, 1991).

Most recently, Grün et al. (2006) conducted a joint U-series/electron spin resonance (ESR) analysis of enamel and dentine fragments from the right $M_3$ of the mandible as well as on the travertine matrix adhering to the mandible. Considerable heterogeneity was seen between the ages derived from the dentine samples, and the mandible appears to have undergone at least two Uranium-accumulation stages (Grün et al., 2006). The travertine samples yielded an age estimate of 42.5 ± 4.1 ka, in good agreement with the results of Julià and Bischoff (1991), whereas the enamel/dentine samples yielded a somewhat older age estimate of 66.0 ± 7.0 ka. This discordance between the enamel/dentine age and the age of the adhering travertine may indicate the mandible was reworked, although Grün et al. (2006) do not favor this hypothesis. Even if it were reworked from the surface of an older travertine, it is unlikely to be more than a few thousand years older than the age of the adhering travertine (Grün et al., 2006). A consensus view, then, would consider the travertine date of Julià and Bischoff (1991) to likely represent a minimum age for the specimen, whereas the enamel/dentine date of Grün et al. (2006) would likely represent close to a maximum age for the specimen. Thus, the age of Banyoles can be considered to fall somewhere between 45 ± 4 ka and 66.0 ± 7.0 ka, and Grün et al. (2006) explicitly rule out the possibility of a late Middle Pleistocene age for the specimen.

### 1.2. The Late Pleistocene evolutionary context of Banyoles

The results of the joint U-series/ESR dating for the mandible from Banyoles place it either in the earlier part of Marine Isotope Stage (MIS) 3 or during MIS 4, when continental glaciation was at its most extensive in the Late Pleistocene. Based on the current fossil record, Europe was occupied solely by Neandertals during the first half of the Late Pleistocene, with *H. sapiens* fossils only appearing during MIS 3 (Ahern et al., 2013; Higham et al., 2014). Although many human fossils do not have a clear chronology, there are very few securely dated fossils from European sites during MIS 4, including perhaps the Neandertal skeleton from Régourdou cave in France (Vandermeersch and Trinkaus, 1995). In contrast, Neandertal remains recovered from sites in southwest

Asia such as Amud, Kebara, and Ein Qashish likely fall between 50 and 70 ka (Schwarcz et al., 1989; Rink et al., 2001; Been et al., 2017), making them potentially contemporaneous with Banyoles, and a similar chronology has been reported for the fossil *H. sapiens* cranium from the site of Manot (Hershkovitz et al., 2015; Alex et al., 2017).

A notable increase in Mousterian occupation sites and Neandertal remains is documented in MIS 3 (Mellars, 1999; Van Andel et al., 2003; Smith et al., 2017), with numerous Neandertal fossils falling within the time range estimated for Banyoles (Higham et al., 2014). However, by around 40 ka, the Neandertals start to disappear from the archaeological and fossil records (Van Andel et al., 2003; Ahern et al., 2013; Smith, 2013; Higham et al., 2014), and the latter half of the Late Pleistocene saw the appearance of *H. sapiens* in Europe.

Although a potentially much earlier *H. sapiens* fossil has been reported from Apidima in Greece by 210 ka (Harvati et al., 2019), the earliest fossil evidence for *H. sapiens* from the Late Pleistocene was recently suggested at the Grotte Mandrin in France dating to between 56.8 and 51.7 ka (Slimak et al., 2022). Other, slightly younger European early *H. sapiens* fossils, include fragmentary specimens from Bacho Kiro cave (Bulgaria; Hublin et al., 2020), a partial cranium from Peştera cu Oase (Romania), some isolated teeth from the Grotta del Cavallo (Italy) and the cranium from Zlatý Kůň (Czechia) and the fragmentary maxilla from Kent's Cavern (England; Benazzi et al., 2011; Higham et al., 2011, 2014; Prüfer et al., 2021). All these early *H. sapiens* specimens likely overlap chronologically with the younger age estimate for Banyoles, and recent genetic evidence suggests that ancestral populations of *H. sapiens* potentially arrived much earlier than MIS 3 (Meyer et al., 2016; Posth et al., 2017; Petr et al., 2020).

Our understanding of the significance of Banyoles has been hampered by several factors. The lack of any archaeological context means behavioral inferences are difficult to draw for this individual, and the precise chronology of the specimen has been an open question for most of the past century. In addition, the extreme tooth wear in this individual also limits useful taxonomic information from the dentition. Fortunately, the chronology of the specimen has much improved, and, although still imprecise, clearly indicates a Late Pleistocene age, likely falling within MIS 3–4. Thus, a Middle Pleistocene age can be ruled out for Banyoles, and this means the most appropriate comparisons for the specimen are with other contemporary hominins in Late Pleistocene Europe and perhaps southwest Asia. As the long and complex history of the taxonomic placement of Banyoles demonstrates, new methodological approaches are necessary to shed further light on this enigmatic specimen.

## 2. Materials and methods

### 2.1. Banyoles preservation and morphology

The mandible is fairly complete but is missing portions of the mandibular rami. The right ramus is missing the upper portion of the coronoid process and the entire condyle, whereas the left ramus is missing most of the superior portion including the condyle, the mandibular notch, and the coronoid process and shows some damage in the gonial region. However, unlike the right ramus, adhering travertine matrix that was not removed from the mandible still preserves a negative impression of the complete posteroinferior aspect of the left condyle in correct anatomical position. This makes it possible to accurately locate the medial and lateral extents of the condyle. The travertine matrix on the left ramus extends inferiorly toward the posterior edge of the alveolar margin, covering the left mandibular foramen internally. The right ramus has remaining travertine on its external aspect extending from the location of the condylar neck anteriorly and inferiorly. Most of the medial face of the ramus, including the mylohyoid groove, is preserved, and the gonial margin is intact. Nevertheless, the remaining travertine effectively separates the coronoid process tip from the rest of the ramus and its current position appears to protrude laterally to an exaggerated extent.

In addition, most of the mandibular corpus is preserved. Unfortunately, accidental damage during the course of study by Hernandez-Pacheco and Obermaier (1915) resulted in some damage and fragmentation of the left corpus as well as damage to the anterior symphysis and misalignment of the anterior dentition, still visible today (Fig. 2). Small pieces of bone are missing along the basal margin near the midline and the left mental foramen. The symphysis itself is fully intact and well-preserved on the internal surface. The external surface is mostly preserved but shows some damage and is represented by three large fragments of bone. The largest fragment preserves most of the anterior surface of the symphysis, but the alveolar margin is damaged. Two smaller fragments are present just inferior to this larger fragment and comprise the inferior aspect of the symphysis. Despite the damage to the left corpus and symphysis, the fragments articulate well between each other, and the current reconstruction seems to accurately reflect the original morphology.

The alveolar margin shows signs of significant resorption and periodontal disease, and the left $M_3$ has been reported to exhibit a carious lesion on the distal aspect (Lalueza et al., 1993). However, the most striking feature of the dentition in Banyoles is the very high degree of dental wear seen on nearly every tooth in the dental arcade (Puech and Puech, 1993). Only the right and left $M_3$s preserve any of the original enamel surface. All the other teeth present a helicoidal wear pattern that is obliquely angled inferiorly and buccally. This is most extreme in the $M_1$s and $M_2$s where the pulp cavity is exposed. Hernandez-Pacheco and Obermaier (1915) and de Lumley (1971–1972) have suggested that the mandible likely represents an older individual based on this severe degree of dental wear. Puech and Puech (1993) suggested that this severe helicoidal dental wear shares similarities with recent *H. sapiens* populations that have an abrasive dried fish diet (Puech and Puech, 1993) as well as similarities with the wear patterns of Andaman islanders, indigenous Australians, and San populations (Lalueza et al., 1993). Lalueza et al. (1993) also noted a small groove on the distal root of the left $M_2$ that may have been from habitual toothpick use.

Given that the damage that occurred to the symphyseal region early on may have obscured some of the chin structures in this individual, it was important to also consult the earliest descriptions of the specimen, before the damage. The earliest description of the mandible describes the symphysis as: "… carecer de apofisis mentoniana a la que sustituye un pequeño y ligero abultamiento discóideo en la parte media de la barba, retirándose luego hacia atras en el borde inferior …" (Alsius, 1915: p. 128), translated as '… lack of a mental process which is replaced by a small and slight discoidal bulge in the middle part of the chin, then retreating backwards at the lower edge …'. This would seem to be describing the presence of a slight symphyseal tubercle or mentum osseum in Banyoles, and the original photographs do show a more projecting inferior margin of the symphysis (Fig. 3).

This same year, Hernandez-Pacheco and Obermaier (1915) published the first detailed description of the specimen, commenting on the damage that occurred to the symphyseal region during the course of their study. Importantly, their morphological observations were carried out before the damage to the specimen. They argue for the presence of a slight mentum osseum along the midline of the symphysis. However, the mental trigone is characterized as barely perceptible, showing at most a

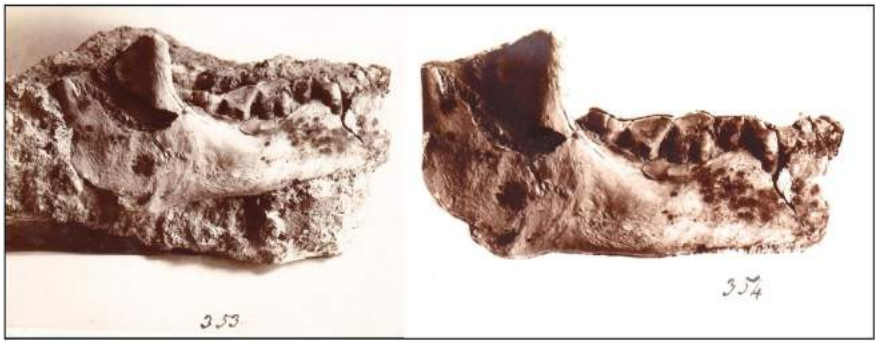


**Figure 3.** Right lateral view of the Banyoles mandible originally published by Alsius (1915; figs. 353 and 354).

very rudimentary form, and Hernandez-Pacheco and Obermaier (1915) argue that the symphyseal morphology in Banyoles represents the earliest stage of evolution of the recent *H. sapiens* chin. Importantly, Hernandez-Pacheco and Obermaier (1915) argue that the damage to the specimen did not alter the symphyseal morphology, as it was possible to perfectly refit the separated pieces back onto the specimen in their original placement. Thus, the current restoration seems fairly close to the original condition of the fossil at the time of discovery.

Subsequent contemporaneous descriptions (MacCurdy, 1915; Bonarelli, 1916; Sergi, 1917) of Banyoles generally agree with the findings of Alsius (1915) and Hernandez-Pacheco and Obermaier (1915). These early accounts both before and just after the damage to the symphysis, agree that Banyoles lacks most of the chin structures seen in living *H. sapiens*, and subsequent studies have largely agreed with this assessment (Dobson and Trinkaus, 2002). However, while de Lumley (1973) and Alcázar de Velasco et al. (2011) later denoted a weakly developed mental fossa on both sides of the anterior symphysis, upon careful examination only a slight depression can be observed on the right side but not on the left.

Furthermore, the internal aspect of the symphysis is fairly vertical but shows a slight expression of an alveolar planum with a shallow genioglossal fossa. Inferiorly, the impressions for the digastric muscles are well-defined and visible when the mandible is viewed in posterior view, suggesting a more posterior orientation also noted by Hernandez-Pacheco and Obermaier (1915).

The dental arcade is parabolic in shape, and the alveolar and basal margins of the mandibular corpus are largely parallel. The position of the mental foramen is under the $P_4$ on both sides and the lateral prominence is located below the distal $M_1$. Internally, the position of the mylohyoid line at the $M_3$ is close to the alveolar margin and angles inferiorly as it moves anteriorly. The distal surface of the $M_3$ is covered by the ramus in lateral view and, thus, there is no retromolar space. A preangular notch is present along the basal margin at the junction of the corpus with the ramus. The gonial margin flares laterally and the insertions for the masseteric muscle are well-defined and visible, especially on the left side. On the internal aspect of the ramus, the mandibular foramen shows the normal morphology, without lingual bridging. A medial pterygoid tubercle is absent on the right side where this region is preserved. The relative heights of the condyle and coronoid process and the shape of the mandibular incisure cannot be determined because of damage to the specimen.

### 2.2. Comparative sample

Banyoles was scanned using computed tomography (CT) by the Institut Català de Paleontologia 3D Virtual Lab at the request of the Alsius family using the following scanning parameters: voltage 200 kV, 3.5 amperage, and a resultant isometric voxel size of 0.25 mm. A 3D model of Banyoles was then generated from the CT scan. The comparative sample included 87 nearly complete adult mandibles (Table 1; Supplementary Online Material [SOM] Table S1). Adult status for the entire comparative sample was determined based on the complete eruption of the $M_3$ (Buikstra and Ubelaker, 1994), and only specimens with a fully erupted $M_3$ were selected for the comparative sample.

The comparative fossil sample included specimens from different geographic regions and chronologies (Table 1). Given the temporal (45–66 ka) and geographic (Western Europe) context associated with Banyoles, the most appropriate comparisons are with Neandertals and fossil *H. sapiens*. We also included five Middle Pleistocene specimens, mainly from Europe, because Banyoles was argued in the past (de Lumley, 1971–1972) to show affinities with European Middle Pleistocene fossils. Microcomputed tomography scans of several fossil specimens ($n = 8$) were obtained from the institutions where the originals are housed (Table 1), and these were used to generate 3D models of the specimens. Three-dimensional models of additional fossil specimens were generated from surface scans of high-quality research casts ($n = 14$) using a NextEngine HD laser scanner and all mandibles were scanned using the same settings (360° rotation, 15 divisions, full high definition, neutral target, and macro range). In addition, 3D models of the Arene Candide mandibles ($n = 4$), generated from surface scans of the original specimens, were retrieved from Morphosource.org. Several fossil specimens that were incomplete were virtually reconstructed (see below).

Finally, the Recent Modern Human (RMH) sample consists of 63 mandibles of unknown sex (Table 1; SOM Table S1). The vast majority of these come from the osteological teaching collection housed at Binghamton University ($n = 36$), as well as eastern European individuals housed at the AMNH (17 female, 9 male). Three-dimensional models of the RMH sample were generated from surface scans using a NextEngine HD laser scanner and the same scanning parameters as for the fossils (see above). Three-dimensional models of two additional RMH individuals were retrieved from online databases (www.morphosource.org; $n = 1$; www.thingiverse.com; $n = 1$).

### 2.3. Data collection

Morphological features This study examined the expressions and frequencies of a series of morphological traits from the mandibular symphysis, corpus, and ramus (Table 2) that are variably expressed in *H. sapiens*, MPE, and Neandertals, and are observable in the mandible from Banyoles (Smith, 1978; Rak et al., 1994; Schwartz and Tattersall, 2000; Quam et al., 2001; Rosas, 2001; Trinkaus et al., 2003; Bermúdez de Castro et al., 2015; Verna et al., 2020). Many of these features (e.g., medial pterygoid tubercle, truncated

**Table 1**
Inventory of the comparative sample used in the present study.

| Specimen | Taxonomic group | Group abbreviation | Geological age | Original/cast | Scan type | Institution scanned |
|---|---|---|---|---|---|---|
| Tighenif 3 | Middle Pleistocene Africa | MPA | 700 ka | Cast | Surface Scan | Binghamton University |
| Arago II | Middle Pleistocene Europe | MPE | 450 ka | Cast | Surface Scan | Binghamton University |
| Arago XIII | Middle Pleistocene Europe | MPE | 450 ka | Cast | Surface Scan | Binghamton University |
| Mauer 1 | Middle Pleistocene Europe | MPE | 600 ka | Cast | Surface Scan | AMNH |
| Montmaurin | Middle Pleistocene Europe | MPE | 190–210 ka | Original | μCT | Musée de l'Homme |
| Amud 1 | *Homo neanderthalensis* | – | 53 ± 8 ka | Original | μCT | Tel Aviv University |
| Kebara 2 | *Homo neanderthalensis* | – | 60 ka | Original | μCT | Tel Aviv University |
| Krapina 59 | *Homo neanderthalensis* | – | 130 ± 10 ka | Cast | Surface Scan | AMNH |
| La Ferrassie 1 | *Homo neanderthalensis* | – | 54–44 ka | Original | μCT | Musée de l'Homme |
| La Quina H5 | *Homo neanderthalensis* | – | 40 ka | Original | μCT | Musée de l'Homme |
| Shanidar 1 | *Homo neanderthalensis* | – | 60 ka | Cast | Surface Scan | AMNH |
| Tabun CII | Early *Homo sapiens* | EMH | 170 ka | Original | μCT | Tel Aviv University |
| Qafzeh 9 | Early *Homo sapiens* | EMH | 120 ka | Cast | Surface Scan | AMNH |
| Skhūl 5 | Early *Homo sapiens* | EMH | 119 ± 18 ka | Cast | Surface Scan | AMNH |
| Abri Pataud | Upper Paleolithic *Homo sapiens* | UPMH | 21 ka | Original | μCT | Musée de l'Homme |
| Brno III | Upper Paleolithic *Homo sapiens* | UPMH | 25 ka | Cast | Surface Scan | AMNH |
| Grotte des Enfants 6 | Upper Paleolithic *Homo sapiens* | UPMH | 28 ka | Cast | Surface Scan | AMNH |
| Ohalo II H2 | Upper Paleolithic *Homo sapiens* | UPMH | 19 ka | Original | μCT | Tel Aviv University |
| Oberkassel 1 | Upper Paleolithic *Homo sapiens* | UPMH | 14 ka | Cast | Surface Scan | AMNH |
| Oberkassel 2 | Upper Paleolithic *Homo sapiens* | UPMH | 14 ka | Cast | Surface Scan | AMNH |
| Arene Candide 1 | Upper Paleolithic *Homo sapiens* | UPMH | 12–14 ka | Original | Surface Scan | Museo Archeologico del Finale/Morphosource |
| Arene Candide 2 | Upper Paleolithic *Homo sapiens* | UPMH | 12–14 ka | Original | Surface Scan | Museo Archeologico del Finale/Morphosource |
| Arene Candide 12 | Upper Paleolithic *Homo sapiens* | UPMH | 12–14 ka | Original | Surface Scan | Museo Archeologico del Finale/Morphosource |
| Arene Candide T4 | Upper Paleolithic *Homo sapiens* | UPMH | 12–14 ka | Original | Surface Scan | Museo Archeologico del Finale/Morphosource |
| Recent modern humans ($n = 63$) | Recent *Homo sapiens* | RMH | Holocene | Originals | Surface Scan | AMNH, (SUNY) Binghamton University, Morphosource, Thingiverse |

AMNH = American Museum of Natural History.

**Table 2**
List of morphological features analyzed in Banyoles and the comparative sample.

| Morphological features | Definition | Possible expressions | Reference |
|---|---|---|---|
| Mentum osseum rank | Development of the chin structures on the anterior surface of the symphysis | Ranks 1–5 | Dobson and Trinkaus (2002) |
| Alveolar planum | Development of the superior aspect of the internal symphysis | Present/absent | Present study |
| Genioglossal fossa | Depression on internal surface for attachment of genioglossal muscles | Shallow/deep | Present study |
| Position of the mental foramen | Horizontal position of the mental foramen relative to the dentition | $P_3/P_4$, $P_4$, $P_4/M_1$, $M_1$, $M_1/M_2$ | Rosas (2001) |
| Retromolar space | Gap between the M3 and anterior ramus margin in lateral view | Absent/present | Franciscus and Trinkaus (1995) |
| Shape of gonial margin | Shape of the posteroinferior margin of the mandibular ramus | Expanded/normal/truncated | Rosas (2001) |
| Masseteric fossa | Depression on the external aspect of the ramus for the insertion of the masseter muscle | Absent/shallow/deep | Rosas (2001) |
| Medial pterygoid tubercle | Presence of a tubercle marking the insertion site of the superior fibers of the medial pterygoid muscle on the internal ramus | Absent/present | Rak et al. (1994); Bermúdez de Castro et al. (2015) |
| Mandibular foramen shape | mandibular foramen showing the normal form or covered by a bridge of bone | Normal/horizontal-oval | Smith (1978); Rosas (2001) |
| Mylohyoid bridging (present/absent) | Presence of a bony covering of the mylohyoid line on the internal aspect of the ramus | Absent/present | Ossenberg (1974); Jidoi et al. (2000) |
| Position of the mylohyoid line at $M_3$ | Vertical position of the mylohyoid line relative to the alveolar margin at the level of the M3 | Low/medium/high | Rosas (2001) |
| Trajectory of mylohyoid line in relation to alveolar margin | Anteroposterior trajectory of the mylohyoid line relative to the alveolar margin | Parallel/irregular/diagonal | Rosas (2001) |

gonion, prominent alveolar planum, horizontal-oval mandibular foramen) are argued to represent derived traits in Neandertals or *H. sapiens*, and their expression in fossil specimens can help to taxonomically classify individuals. Although Banyoles is fairly complete, some features of the ascending ramus could not be included because of the preservation of the specimen. In addition, the heavily worn state of the dentition largely limits any observations to those based on the root morphology.

Expression of a chin followed the ranking system developed by Dobson and Trinkaus (2002). This scoring system ranks mentum osseum development from 1 to 5, where a rank of 1 indicates the "complete absence of a mentum osseum with posteroinferior rounding of the anterior symphysis" (Dobson and Trinkaus, 2002: 73) and a rank of 5 indicates the "strong presence of a mentum osseum with prominent tuberculum laterale and the formation of a projecting, shelf-like anteroinferior border to the symphysis"

(Dobson and Trinkaus, 2002: 74). In the present study, ranks 1–3 were taken to reflect the absence of a mentum osseum, while a mentum osseum was considered present for ranks 4–5. Dobson and Trinkaus (2002) have previously assigned the Banyoles mandible a mentum osseum rank of 1, indicating no development of any relief on the external symphysis.

Virtual reconstruction We performed a virtual reconstruction of Banyoles, based on mirror-imaging across the sagittal plane, to complete some damaged sections of the ascending ramus using Mimics v. 20.0 (Materialise Mimics, Belgium). In particular, the left condylar region was mirror-imaged to the right side and the right gonial margin was mirror-imaged to the left side. This made it possible to include a series of landmarks on the nearly complete mandible in the 3D GM analysis. Additional fossil specimens were virtually reconstructed by mirror-imaging one side of the mandible to the other if the specimen was incomplete but preserved the midline sagittal plane. Virtual reconstruction for this study was adapted from protocols for 3D reconstruction outlined by Benazzi et al. (2009) and Weber and Bookstein (2011).

First, three separate reconstructions were generated for Banyoles to control for potential intraobserver error in the reconstruction process. Each of the reconstructions was made on a separate day and was thresholded relying on the standard half-maximum height protocol (Weber and Bookstein, 2011). Subsequently, a 3D model of the mandible was produced through two processes: global alignment and manual local positioning (Fig. 4). The first step in global alignment is to place bilateral landmarks on the mandibular corpus and ramus. The specimen is then mirror-imaged about the midline and the homologous bilateral landmarks are aligned to yield a best fit. This results in an estimation of the location of any missing portions on one side of the mandible. In the case of Banyoles, both the right and left condyles are not preserved. Nevertheless, a negative impression of the posterior surface of the left condyle in correct anatomical position is preserved within the adhering travertine on the posterior aspect of the ramus. Thus, the travertine was not virtually removed, but was used in the mirror-imaging to place the right condyle in the virtual reconstruction. After the global alignment is completed, manual local alignment is performed to align the mirrored left ramus with the right ramus. After the two objects are aligned, they are then fused together into a single 3D model. These steps were repeated for several additional fossil mandibles that needed to be reconstructed. The following specimens were all virtually reconstructed using the mirror image reconstruction techniques described earlier: Arago II, Arago XIII, Kebara 2, La Quina H5, Qafzeh 9, and one RMH (Bio B).

### 2.4. Data analysis

Landmark placement Three-dimensional geometric morphometrics was carried out to compare Banyoles with the comparative sample. We included 22 landmarks, or 3D points, that best capture the overall shape of Banyoles (Fig. 5; SOM Table S2). Landmarking of all the fossil and recent individuals in this study was performed by the first author. Landmarking of all mandibles were performed using the Mimics Medical v. 20.0 landmarking tool. These landmarks are based on standard osteometric points of the mandible and have been used by other researchers in earlier studies (Rosas and Bastir, 2002, 2004; Nicholson and Harvati, 2006; Rosas et al., 2019). Some landmarks were not included (e.g., tip of coronoid process) if they were not preserved in Banyoles.

Three-dimensional geometric morphometrics Landmarks were subjected to a Generalized Procrustes Analysis (GPA) using MorphoJ v. 1.08.0 (Klingenberg, 2011), resulting in a new set of Procrustes-fitted coordinates. This involves calculating the centroid point of all landmarks in a configuration for each individual within the comparative sample and subsequently

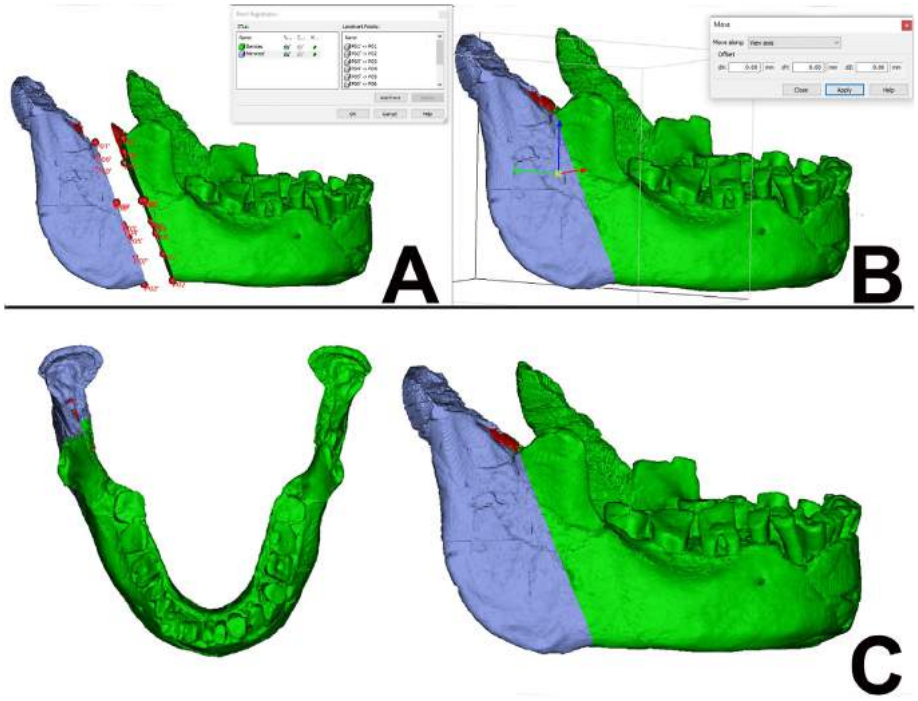


**Figure 4.** Reconstruction process of a 3D model of the Banyoles mandible. A) Right lateral view of the Banyoles mandible during the global alignment process. The red dots indicate pairs of landmarks used to align each piece of the mandible to each other. B) Right lateral view of the Banyoles mandible after reconstruction and global alignment. The blue, green, and red arrows indicate manual mode where the user manually moves each object together. C) Superior view (left) and right lateral view (right) of the Banyoles mandible after mirroring the right condyle. Highlighted piece in blue indicates mirrored element. (For interpretation of the references to color in this figure legend, the reader is referred to the Web version of this article).

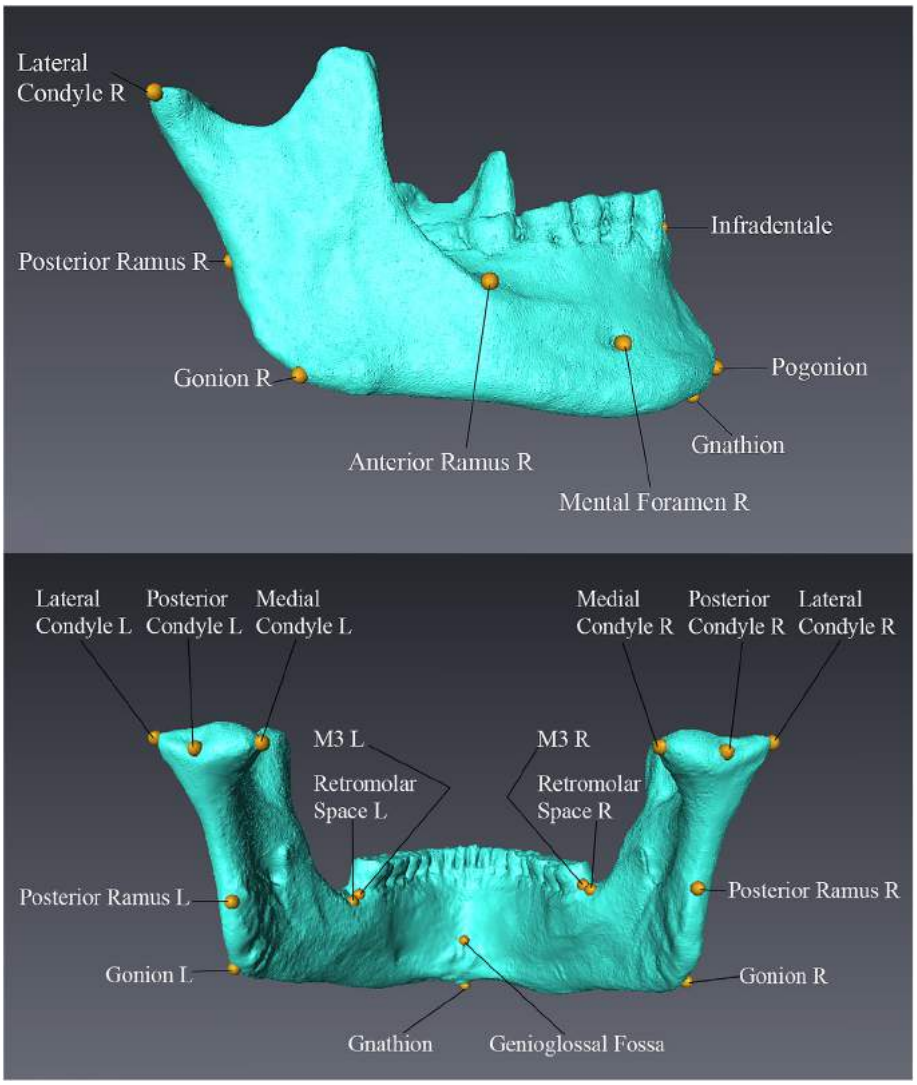


**Figure 5.** Locations of the landmarks used in this study on a modern human mandible (BU 21). Landmarks were placed in Avizo v. 7.0 for visualization and processed in Photoshop v. 23.1.0. Top image, right lateral view of the mandible. Bottom image, posterior view of the mandible.

translating each of these centroids to a single origin point in 3D. These Procrustes coordinates are then scaled to reflect the removal of size (but not necessarily shape variation related to allometry), and then are rotated to minimize the sum of squared distances between them. Size is retained as a separate variable, centroid size. To assess which landmarks explain the most variation within the sample, a principal component analysis (PCA) was computed in MorphoJ v. 1.08.0. An assessment of the shape variance represented by each principal component (PC) axis was carried out with R v. 4.2.1 in RStudio 2022.02.1+461 using the 'warpRefMesh' function in the 'Geomorph' package (R Core Team, 2022; RStudio Team, 2022; Adams and Otárola-Castillo, 2013; Baken et al., 2021). This involved identifying the RMH mandible (DU_EA_CH01) closest to the origin point (0,0) on the PCA bivariate plot showing the sample specimens along the PC1 and PC2 axes, and then warping it to the predicted origin shape. The starting shape mandible was then further warped to the Procrustes fitted coordinates that represent the extreme value along each PC axis. Three Pleistocene individuals were not included in the 3D GM analysis—the Neandertal specimen Kebara 2 and the Pleistocene *H. sapiens* specimen Brno III due to distortion issues, and KNM-BK 67, which was missing both gonial regions.

In addition, we statistically evaluated whether the position of each reconstruction of Banyoles based on the first two PCs is significantly different (i.e., how dissimilar) from any of the five comparative groups (i.e., RMH, MPE, Neandertals, EMH, and UPMH). First, we generated the centroid coordinate (i.e., the geometric mean for each PC) of each group (including the centroid between all three reconstructions of Banyoles) in the PCA bivariate plot. Then, we measured the Euclidean distances between the centroid of the three Banyoles reconstructions and each group centroid using the 'dist2centroid' function from the 'swaRm' package (Garnier, 2021) with R v. 4.2.1 in RStudio 2022.02.1+461. Similarly, we calculated the Euclidean distances of each member in a group to their respective group centroid as well as each Banyoles reconstruction to that respective group centroid for further statistical analysis.

We conducted a Welch's t-test, which is more robust compared to a Student's t-test (see Delacre et al., 2017), to test for statistical significance. We conducted five (i.e., one for each group in the comparative sample) permuted ($n$ = 10,000) two-sample tests. Welch's t-test was computed between the Euclidean distances of each member of a group and each reconstruction of Banyoles to the group's centroid. The permutation analysis used a resampling without replacement approach by identifying all the different

combinations of individuals into the groups being compared (see Kohl, 2020). The null hypothesis is that the group that is not significantly different from the three reconstructions of Banyoles is likely the taxonomic group that Banyoles is most similar to in the first two PCs. For example, we performed a permuted ($n = 10{,}000$) Welch's t-test comparing how different the Euclidean distances of the Banyoles reconstructions (i.e., distances between the three reconstructions of the Banyoles mandible to the RMH group centroid) are to the Euclidean distances of the RMH group (i.e., distances of members in the RMH group to their group centroid). All five permuted Welch's t-tests were performed using the 'MKinfer' package (Kohl, 2020) with an a priori alpha level of significance set to $p < 0.05$. All statistical analyses and packages were performed using R v. 4.2.1 (R Core Team, 2022) through RStudio 2022.02.1+461 (RStudio Team, 2022).

Furthermore, we also statistically evaluated whether the set of Procrustes fitted landmarks from the reconstructions of Banyoles is significantly different (i.e., how dissimilar) from any of the five comparative groups (i.e., RMH, MPE, Neandertals, EMH, and UPMH) when considering total shape variation as opposed to only the first two PCs. We performed a permuted ($n = 10{,}000$) canonical variate analysis (CVA) which calculated Procrustes distances between each of the comparative groups to the reconstructions of Banyoles. The permuted CVA was computed in MorphoJ v. 1.08.0 (Klingenberg, 2011) with an a priori alpha level of significance set to $p < 0.05$.

Furthermore, the effects of allometry (i.e., the relationship of size on shape) were also tested through both simple linear and multivariate regression. Simple linear regression involved regressing PC scores from the top five PC axes on the natural log of centroid size; this provided some estimate of how these individual PC axes were related to size. Multivariate regression involved regressing the Procrustes residuals for each individual on the natural log of centroid size; in contrast to the univariate regression, this provides a global measure of how size and shape are related in the entire sample. All regression analyses were permuted ($n = 10{,}000$) involving randomly generated reassignment of observations of the dependent variables and were computed in MorphoJ v. 1.08.0 using the regression function.

Intraobserver error estimation We performed an intraobserver error analysis of the landmarks used in this study as well as the landmarks from three reconstructions of Banyoles following the protocols outlined in Shearer et al. (2017), to ensure that our results reflect the true biological signal of variation rather than error in landmark placement and also on the reproducibility of the virtual reconstructions. We calculated the average Procrustes distance for all landmarks in 10 copies of the same RMH individual (VL 2609a; hereafter referred to as the 'replicates' group) and in 10 different RMH individuals (BU 1, BU 2, BU 3, BU 4, BU 5, BU 6, BU 7, BU 8, BU 9, and BU 10b; hereafter referred to as the 'different' group). A two-sample Welch's t-test was then performed using R v. 4.2.1 (R Core Team, 2022) through RStudio 2022.02.1+461 (RStudio Team, 2022) to establish whether the means of these two groups were statistically different ($p < 0.05$). If the average Procrustes distance in the replicates group is significantly smaller than that in the different group, then there is no intraobserver bias in landmark placement. Similarly, we computed two Welch's two-sample t-tests between the three Banyoles reconstructions and the replicate RMH group and the different RMH group. If the average Procrustes distance in the Banyoles reconstructions is statistically indistinguishable from the replicates RMH group but statistically different from the different RMH group, we can have more confidence in the reproducibility of the Banyoles reconstructions. This is because the virtual reconstructions should be nearly identical and thus the mean Procrustes distances should be no different than that of repeatedly landmarking the same mandible.

## 3. Results

### 3.1. Comparative morphological analysis

Mandibular symphysis Banyoles shows a fairly vertical symphysis (94°), without an incurvatio mandibulae anterior but showing a weak expression of a lateral tubercle and possible mental fossa on the right side. Thus, we agree with Dobson and Trinkaus (2002) assigning a mentum osseum rank of 1 to Banyoles (Table 3). Although Alcázar de Velasco et al. (2011) suggested that Banyoles may have a mental trigone, the full suite of features found in RMH is not present, and Banyoles retains the primitive condition of a low mentum osseum rank. Comparison of the mentum osseum rank in Banyoles with other Pleistocene and recent *Homo* specimens (Table 3) shows that Banyoles shared the expression most frequently seen in MPEs as well as some Neandertals.

The presence of a superior transverse torus is an archaic feature in the genus *Homo*, represented by a swelling of bone on the internal aspect of the symphysis. When present, the superior transverse torus also creates an alveolar planum, an obliquely sloped surface just posterior to the dentition representing the superior aspect of the torus. The torus is demarcated inferiorly by the presence of the genioglossal fossa, the insertion site for the genioglossal and geniohyoid muscles. When observing the expression in Banyoles, the posterior symphysis is fairly vertical, suggesting, at most, only a slight alveolar planum and a relatively shallow genioglossal fossa. The presence of a developed superior transverse torus and genioglossal fossa is considered a primitive feature within the genus *Homo* and characterizes European Middle Pleistocene specimens and Neandertals (Quam et al., 2001; Daura et al., 2005; Carbonell et al., 2008; Bermúdez de Castro et al., 2010; Vialet et al., 2018). In contrast, RMH generally lacks a superior transverse torus and genioglossal fossa, showing a fairly vertical internal symphysis with, at most, some expression of genial tubercles (Daegling, 2005; Lipski et al., 2013).

Along the basal border of the mandibular symphysis, the digastric fossae mark an origin site of the anterior belly of the digastric muscles to a fibrous tendon attached to the hyoid bone and another origin of the posterior belly of the mastoid, or styloid, process on the temporal bone (De-Ary-Pires et al., 2003). The orientation and morphology of the digastric fossae on Banyoles presents a posteriorly oriented digastric fossae with a well-marked muscle site attachment. This is similar to the more derived

**Table 3**
Mentum osseum ranks for the Banyoles mandible compared with Pleistocene and recent modern humans.

| Specimen/group | *n* | Mentum osseum rank | | | | | Source |
|---|---|---|---|---|---|---|---|
| | | 1 | 2 | 3 | 4 | 5 | |
| Banyoles | | X | | | | | Present study |
| Middle Pleistocene Europe | 10 | 70% | 30% | | | | Dobson and Trinkaus (2002); includes Arago 13 (rank = 1) |
| Neandertals | 18 | 28% | 44% | 28% | | | Dobson and Trinkaus (2002) |
| Pleistocene modern humans | 14 | | | | 64% | 36% | Dobson and Trinkaus (2002) |
| Recent modern humans | 63 | | | | 38% | 62% | Present study |

posterior orientation seen in RMH and in contrast to the primitive inferior condition seen in MPE and Neandertal fossil mandibles (Liu et al., 2010; Hershkovitz et al., 2021).

Mandibular corpus The position of the mental foramen in relation to the tooth row has long figured in descriptions of Pleistocene *Homo* mandibles. In Banyoles, the mental foramen is located directly under the $P_4$ (Table 4), resembling the placement in RMH and early *Homo* specimens (Rosas, 2001). In contrast, a relatively posterior placement, frequently located under the $M_1$, in Neandertals (Table 4) is considered to represent a derived condition that reflects the development of midfacial prognathism in this group of hominins (Stringer et al., 1984; Trinkaus, 1987; Rosas, 2001). This posterior position is also commonly found in MPE mandibles. On the other hand, earlier *Homo* fossils such as *Homo habilis*, *Homo ergaster*, and *Homo erectus* generally show a more anterior placement of the foramen under the $P_3$ or $P_4$ (Rosas and Bermúdez de Castro, 1998; Rosas, 2001; Carbonell et al., 2005; Bermúdez de Castro et al., 2007; Carbonell et al., 2008). Also, this study (Table 4) suggests *H. sapiens* show this more anterior placement, indicating they show the primitive condition for the genus *Homo* in this feature. The retromolar space is represented by a gap in lateral view between the anterior ramus margin and the posterior edge of the third molar (Franciscus and Trinkaus, 1995) and has been regarded as a derived feature of Neandertals, one that was also present in European Middle Pleistocene specimens (Stringer et al., 1984; Rak, 1986; Creed-Miles et al., 1996; Rosas, 2001; Smith, 2013). Neandertals show the highest frequency of a retromolar space (81%), and this feature was also present in over half (53%) of European Middle Pleistocene specimens (Table 5). It occurs at lower frequencies in fossil and recent *H. sapiens* mandibles, which usually lack a retromolar space. Its absence in African Middle Pleistocene mandibles as well as Asian *H. erectus* specimens suggests this represents the primitive condition for the genus *Homo* (Franciscus and Trinkaus, 1995). In Banyoles, the anterior ramus margin overlaps with the posterior aspect of the $M_3$, indicating the absence of a retromolar space, and resembling early *Homo* specimens as well as in RMH.

On the internal aspect of the mandibular corpus, variation in the position of the mylohyoid line relative to the alveolar margin at the level of the $M_3$ has been observed in different species within the genus *Homo* (Table 6; Rosas, 2001). Earlier members of the genus *Homo* tend to show a relatively low position of the mylohyoid line at the level of the $M_3$, being located clearly below the alveolar margin (Rosas, 2001). This same condition is generally seen in European Middle Pleistocene specimens. In contrast, Neandertals mainly show a higher position of the mylohyoid line, being located very close to the alveolar margin at the $M_3$ and a steeply inclined diagonal trajectory of the mylohyoid line, descending anteriorly (Rosas, 2001). In Banyoles, the mylohyoid line is not located close to the alveolar margin and the inclination anteriorly is not steep. In both these features, Banyoles differs from Neandertals but resembles the European Middle Pleistocene specimens and our recent human sample (Table 6).

Mandibular ramus The preangular notch is a feature located along the basal margin of the mandibular ramus, just anterior to gonion, and is produced by an expansion of the gonial region. A normal gonial profile follows a smooth curve from the inferior corpus to the posterior ramus giving it a rounded profile. Variation in the shape of the gonial region in the genus *Homo* has been previously described, with a normal or slightly expanded gonial region seen in RMH and some fossil specimens (e.g., Zhoukoudian G1, KNM-ER 992; Weidenreich, 1936; Wood, 1991) apparently being considered the primitive morphology for the genus (Rosas 2001). In contrast, the gonial margin has a unique expression in Neandertals where a truncated gonial profile is often seen and the "gonion angle is formed as a third arista between the posterior border of the ramus and the basal border" (Creed-Miles et al., 1996:152). Specimens that show this truncated morphology also generally lack a preangular notch. The majority (80%) of the MPE fossils (except for Mauer and Arago 13) show a normal, rounded gonial margin, whereas 75% of Neandertals had a truncated gonion, supporting the suggestion of Rosas (2001) that this represents a derived Neandertal feature (see also Table 7). In our RMH sample, 76% have an expanded gonion, with 24% of them having a rounded gonial profile, and none having a truncated gonion. The expanded gonial profile in Banyoles, clearly seen on the well-preserved right side, is most similar to early *Homo* specimens and RMH which clearly differ from the Neandertal expression.

The masseteric fossa is a variable depression on the external aspect of the ramus and is related to the strength of attachment of the masseter muscle at the gonial region of the mandible (Spencer and Demes 1993; Rosas 2001). Rosas (2001) previously recorded three expressions (deep, shallow, and flat) of this feature in the genus *Homo*. A deep masseteric fossa is created when the gonial region flares out laterally creating a deep depression. A shallow masseteric fossa is when the outline of the depression can be macroscopically observed but is not as pronounced. Finally, in the flat expression, individuals do not show any lateral flaring from the masseter muscle, and sometimes express a slight indentation of the gonial region. Among European Middle Pleistocene specimens, 74%

**Table 4**
Position of the mental foramen in Banyoles compared with Pleistocene and recent modern humans.

| Specimen/Group | *n* | $P_3/P_4$ | $P_4$ | $P_4/M_1$ | $M_1$ | Source |
|---|---|---|---|---|---|---|
| Banyoles | | | X | | | Present study |
| Middle Pleistocene Europe | 20 | 0% | 15% | 45% | 40% | Trinkaus and Shipman (1993); Rosas (2001) |
| Neandertals | 25 | 0% | 4% | 32% | 64% | Trinkaus and Shipman (1993) |
| Recent modern humans | 75 | 15% | 76% | 9% | | Present study |

**Table 5**
Retromolar space expression in the Banyoles mandible compared with Pleistocene and recent modern humans.

| Specimen/Group | *n* | Present | Absent | Source |
|---|---|---|---|---|
| Banyoles | | | X | Present study |
| Middle Pleistocene Europe | 15 | 53% | 47% | Franciscus and Trinkaus (1995); Rosas (2001) |
| Neandertals | 32 | 81% | 19% | Franciscus and Trinkaus (1995) |
| Pleistocene modern humans | 29 | 28% | 72% | Franciscus and Trinkaus (1995) |
| Recent modern humans | 59 | 31% | 69% | Present study |

**Table 6**
Position of the mylohyoid line at $M^3$ in the Banyoles mandible compared with Pleistocene and recent humans.

| Specimen/sample | *n* | Low | Medium | High | Source |
|---|---|---|---|---|---|
| Banyoles | | X | | | Present study |
| Middle Pleistocene Europe | 15 | 93% | 7% | 0% | Rosas (2001) |
| Neandertals | 28 | 14% | 32% | 54% | Rosas (2001) |
| Recent modern humans | 70 | 57% | 29% | 14% | Present study |

**Table 7**
Morphology of the gonial region in the Banyoles mandible compared with Pleistocene and recent humans.

| Specimen/group | *n* | Expanded | Normal | Truncated | Source |
|---|---|---|---|---|---|
| Banyoles | | X | | | Present study |
| Middle Pleistocene Europe | 10 | | 80% | 20% | Rosas (2001) |
| Neandertal[a] | 12 | | 25% | 75% | Rosas (2001) |
| Recent modern humans | 75 | 76% | 24% | | Present study |

[a] Krapina J, Shanidar 1, Le Moustier 1.

of individuals had a deep masseteric fossa, and a few shared the other two expressions (Table 8). A deep fossa characterizes the Sima de los Huesos mandibles as well as Arago 13. In contrast, most Neandertals (82%) have a flat masseteric region, with only 18% showing a shallow depression and none showing a deep fossa (Table 8). In our RMH sample, the majority of individuals (57%) have a deep masseteric fossa while nearly a third (37%) show a shallow fossa and a fossa is absent in only 5% of individuals (Table 8). The deep masseteric fossa in Banyoles is an expression shared with European Middle Pleistocene fossils and *H. sapiens*.

The medial pterygoid tubercle is located on the internal aspect of the ramus and reflects a hypertrophy of the superior fibers of the medial pterygoid muscle. Individuals that lack a masseteric fossa on the external ramus generally also have pronounced pterygoid muscle attachments on the medial ramus (Rosas, 2001). This tubercle has been argued previously to be a derived trait of Neandertals (Rak et al., 1994; Trinkaus, 2006), and it does occur at high frequencies (94%) in this group, as well as in approximately half (53%) of European Middle Pleistocene fossils (Bermúdez de Castro et al., 2015). In contrast, the majority (ca. 75%) of RMH lack a medial pterygoid tubercle (Bermúdez de Castro et al., 2015), and a clear tubercle was similarly absent in 89% of the RMH sample in the present study. The internal aspect of the right ramus in Banyoles is well preserved and shows several muscle markings for the insertion of the medial pterygoid muscle. However, no medial pterygoid tubercle is present superiorly (contra Alcázar de Velasco et al., 2011), and its absence in Banyoles distinguishes it from Neandertals.

The mandibular foramen is located on the internal aspect of the ramus and transmits the mandibular branch of the fifth cranial nerve (CN V). In RMH, the foramen is usually partially covered by the lingula, which is open posteriorly, and connects directly to the mylohyoid groove. In contrast, a distinct horizontal-oval (H-O) morphology of the foramen has been noted in Neandertals, which often show a lingula that completely encompasses the canal and separates it from the mylohyoid groove (Smith, 1978). Although this feature has not been systematically reported in the literature for fossils outside of Europe, data for Neandertals suggest the H-O form is present in just under 50% of Neandertal individuals (Smith, 1978; Stefan and Trinkaus, 1998), but is mainly absent in European Middle Pleistocene specimens. A very low frequency of this feature (ca. 3%) has been reported in RMH (Table 9). Banyoles expresses the ancestral (i.e., not the H-O form) state of the mandibular foramen on the right ramus where it can be clearly observed, differing from the majority of Neandertals.

Occasionally, a bony bridge of bone (mylohyoid bridge), partially covering the mylohyoid groove, is present on the internal ramus. Recent modern humans generally lack mylohyoid bridging, and a study of this feature in a large sample of recent humans reported a relatively low frequency (13%) of occurrence when compared to Neandertals (Ossenberg, 1974). Approximately half of Neandertals (52%) show some form of bridging of the mylohyoid groove, and the presence of bridging has been positively correlated with the H-O form of the mandibular foramen (Jidoi et al., 2000). Similarly, 50% of a small European Middle Pleistocene sample in this study showed some degree

**Table 8**
Expression of the masseteric fossa in the Banyoles mandible compared with Pleistocene and recent humans.

| Specimen/sample | *n* | Deep | Shallow | Flat | Source |
|---|---|---|---|---|---|
| Banyoles | | X | | | Present study |
| Middle Pleistocene Europe | 15 | 74% | 13% | 13% | Rosas (2001) |
| *Homo* neanderthalensis | 22 | | 18% | 82% | Rosas (2001) |
| *Homo* sapiens | 74 | 57% | 37% | 5% | Present study |

**Table 10**
Mylohyoid bridging in the Banyoles mandible compared with Pleistocene and recent humans.

| Specimen/Sample | *n* | Present | Absent | Source |
|---|---|---|---|---|
| Banyoles | | | X | Present study |
| Middle Pleistocene Europe | 4 | 50% | 50% | Present study |
| Neandertals | 29 | 52% | 48% | Jidoi et al. (2000) |
| Recent humans | 7811 | 13% | 87% | Ossenberg (1974) |

**Table 9**
Mandibular foramen morphology in the Banyoles mandible compared with Pleistocene and recent humans.

| Specimen/sample | *n* | Normal | Horizontal - Oval | Source |
|---|---|---|---|---|
| Banyoles | | X | | Present study |
| Middle Pleistocene Europe | 12 | 100% | 0% | Smith (1978); Stefan and Trinkaus (1998) |
| Neandertals | 27 | 56% | 44% | Smith (1978); Stefan and Trinkaus (1998) |
| Recent humans | 478 | 97% | 3% | Smith (1978); Stefan and Trinkaus (1998) |

of bridging, as seen in Mauer and Montmaurin (Table 10). The right ramus of Banyoles, where the mylohyoid groove is well-preserved and can be seen in its entirety, shows no evidence of bridging.

### 3.2. Intraobserver error

The average Procrustes distance was calculated for all the landmarks in 10 copies of the same RMH individual and in 10 different RMHs (SOM Table S3). The mean Procrustes distance for the three Banyoles reconstructions was similar to that of the replicated RMH sample and the values for all three Banyoles reconstructions clearly fall within the range of variation of the replicate RMH sample. The mean Procrustes distance of the three Banyoles reconstructions (SOM Table S3) was significantly lower ($p < 0.0001$) than the 10 different RMH individuals. In contrast, no difference ($p = 0.58$) was found in the Procrustes distances between the RMH replicate sample and the Banyoles replicate sample. We found a significantly smaller Procrustes distance ($p < 0.0001$) in the sample consisting of copies of the same individual (SOM Table S3), indicating that the intraobserver error in landmark placement is lower than the true biological signal.

Thus, these results indicate two important things. First, that the intraobserver error in the Banyoles replicates resembles that seen in the RMH replicate sample, giving credence to the reliability of the reconstructions. Second, the downstream 3D GM analysis that includes all the comparative specimens has minimized the error in landmark placement to better reflect a biological signal of variation.

### 3.3. Three-dimensional geometric morphometric analysis

The PCA generated 64 PCs that explain 100% of the shape variance. The first two PCs explain just under half (45.63%) of the total variance (Table 11) and reveal separation between some groups. Principal components 3–5 represent a total of 22.83% of the total shape variation but did not reveal any taxonomic separation. Principal component 3 reflects changes in the flexure of the ramus where positive PC3 scores equate to a more posteriorly flexed condylar region, anterior migration of the posterior ramus, and superoanterior migration of gonion while negative scores equate to a less posteriorly flexed condylar region, a posterior migration of the posterior ramus, and an inferoposterior migration of gonion. Principal component 4 primarily reflects shape changes in the condylar neck and migration of the dentition. Positive PC4 scores indicate a posterior migration of the dental arcade, a superior position of pogonion, and a shorter condylar neck, whereas negative scores reflect an anterior migration of the dental arcade, an inferior position of pogonion, and a taller condylar neck. Principal component 5 reflects shape changes in the depth of the mandibular corpus where positive scores indicate a deeper corpus and negative scores reflect a shallower corpus. No other combinations of PCs revealed

**Table 11**
Results of the top five principal components from the principal component analysis.

| PC | Eigenvalues | % Variance | Cumulative % | % Variance explained by Allometry |
|---|---|---|---|---|
| 1 | 0.00206373 | 29.779 | 29.779 | 0.00% |
| 2 | 0.00109862 | 15.853 | 45.631 | 19.21% |
| 3 | 0.0007229 | 10.431 | 56.063 | 8.58% |
| 4 | 0.00047668 | 6.878 | 62.941 | 0.11% |
| 5 | 0.00038228 | 5.516 | 68.457 | 0.00% |

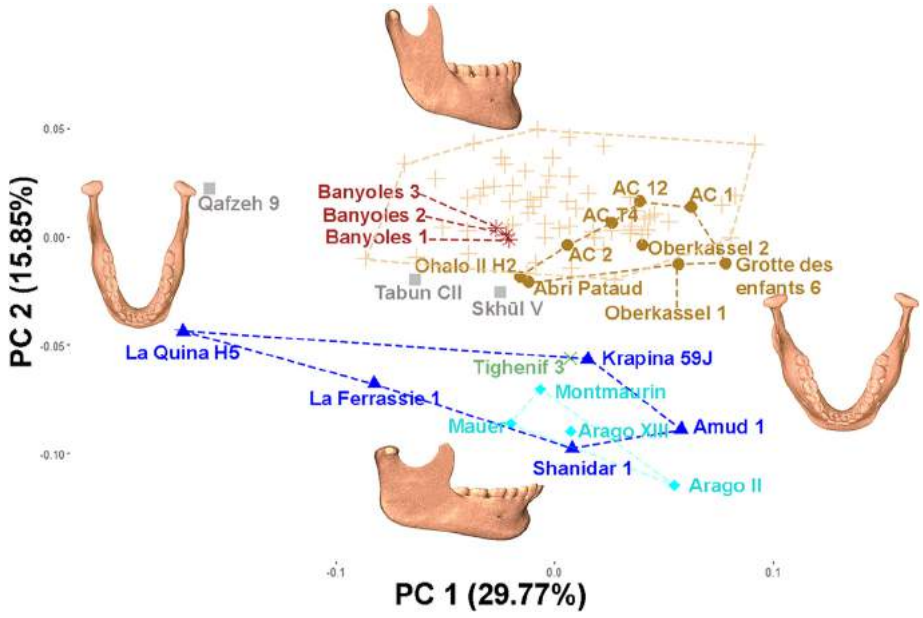


**Figure 6.** Plot of the first two principal components (PCs) from a PC analysis of the Procrustes landmarks (see also Table 11). The extremes of shape variation along each axis are shown by warping a modern human mandible (DU_EA_CH01). Banyoles reconstructions = red stars, recent modern humans (RMH) = tan crosses, Upper Paleolithic modern humans (UPMH) = brown circles, early modern humans (EMH) = gray squares, Neandertal = blue triangles, Middle Pleistocene Europeans (MPE) = cyan diamonds, Middle Pleistocene African = green 'X'. Figure was generated using the PC scores using R v. 4.2.1 in Rstudio 2022.02.1+461 using the 'ggplot2' package (Wickham, 2009) and superimposed warped mandibles using R v. 4.2.1 in RStudio 2022.02.1+461 using Photoshop v. 23.1.0. (For interpretation of the references to color in this figure legend, the reader is referred to the Web version of this article).

any further taxonomic separation and therefore only PC1 and PC2 were examined further for taxonomic assessments.

Principal component 1 mainly reflects variation in the overall widths of the mandible. Specimens with negative scores along PC1 (e.g., La Quina H5) represent a narrower U-shaped mandible, and specimens with positive scores along PC1 (e.g., Grotte des Enfants 6) represent a wider arch-shaped mandible (Fig. 6). Principal component 2 reflects variation in the gonial profile, ramus morphology, mental foramen position, symphyseal region, and overall shape of the dental arcade. Specimens with positive scores along PC2 (e.g., many of the recent *H. sapiens* specimens) tend to have an expanded and laterally flaring gonial profile, an anteroposteriorly (AP) narrower ramus, more anterior mental foramen position, an AP shorter dental arcade, and a more anteriorly projecting external symphysis. Whereas specimens with negative scores along PC2 (e.g., Arago II) have a truncated gonial profile with no lateral flaring, an AP wider ramus, posteriorly oriented mental foramen, an AP longer dental arcade, and a more retreating symphyseal region.

The PCA revealed a clear separation along PC2 between the Neandertals and MPE specimens on the one hand, and *H. sapiens* on the other (Fig. 6). Pleistocene and recent *H. sapiens* show largely positive values on PC2, while the archaic *Homo* specimens, including the Neandertals, showed uniformly negative values, with only limited overlap between the modern and non-modern groups. The MPE specimens tend to cluster together with the Neandertals and the MPA specimen Tighenif 3 in shape space. One of the Neandertals (La Quina H5) fell further away from most Middle-to-Late Pleistocene *Homo* specimens along PC1, reflecting its narrower dental arch. All three reconstructions of Banyoles fell very close to one another and are clearly within the recent *H. sapiens* grouping along PC1 and PC2. The three nearest neighbors to Banyoles based on Euclidean distances are all RMH individuals, while the three nearest fossil specimens (AC 10997, Ohalo 2 H2, Abri Pataud) are all UPMH, with Ohalo II H2 being the closest fossil specimen to Banyoles.

Evaluating the Euclidean distances from the centroid of the Banyoles reconstructions to each group's centroid along PC1 and PC2 (Table 12) further revealed that Banyoles falls closest to the centroid of the RMH sample, followed by the EMH and UPMH groups. The Neandertals and MPE centroids fell further away from Banyoles. The results of the Welch's t-test demonstrated that the mean of the three Banyoles reconstructions to the centroids of all groups except RMH were statistically significant ($p < 0.05$), indicating that Banyoles is morphologically closest to RMH individuals (Table 12).

Comparing the CVA results based on the Procrustes distances from reconstructions of Banyoles to each group (Table 13) revealed that Banyoles falls closest to the centroid of the UPMH sample, followed by the RMH and EMH groups. The Neandertals and MPE group fall furthest away from Banyoles based on their Procrustes distances. However, the Procrustes distance from the reconstructions of Banyoles to each group were all statistically significant ($p < 0.05$; Table 13). This suggests that while the reconstructions of Banyoles are squarely within the range of variation of the RMH group based on the first two PCs, the reconstructions of Banyoles are still significantly different from each group when considering total shape variation.

The effects of allometry on the Procrustes residuals were relatively small, with allometry accounting for only 4.283% of the variation (SOM Table S4). Shape variation explained by each PC was also relatively small overall but still statistically significant (SOM Table S4). The percentage of shape variation explained by allometry is 0.003% ($p = 0.953$) in PC1 but 19.21% ($p < 0.001$) in PC2. Allometry explains 8.58% of the total shape variation represented in PC3 ($p < 0.001$) but less than 1% in PC4 and PC5.

## 4. Discussion

The comparative morphological analysis of Banyoles revealed that this fossil specimen shows several features that are likely primitive expressions for the genus *Homo*. These include the low mentum osseum rank and lack of chin structures, the relatively anterior placement of the mental foramen under the $P_4$ and lack of a retromolar space as well as an expanded gonial margin, the absence of a medial pterygoid tubercle and the normal mandibular foramen morphology in the ramus. Other features are either more ambiguous in their phylogenetic polarity or their expression in Banyoles is somewhat intermediate, including the alveolar planum development, the mylohyoid line position at the $M_3$, the deep masseteric fossa and the absence of lingual bridging of the mylohyoid groove. The expression of these morphological

**Table 12**
Results of the pairwise permuted Welch's *t*-tests comparing the mean Euclidean distances in the Banyoles reconstructions to the mean Euclidean distance in each group.

| Groups compared | Distance to Group Centroid | t-value | s | *p*-value[a] | Permutations | Permutated *p*-value[a] |
|---|---|---|---|---|---|---|
| Banyoles and RMH | 0.03 | 2.022 | 0.003 | 0.048* | 10000 | 0.139 |
| Banyoles and UPMH | 0.05 | −6.38 | 0.003 | <0.001*** | 10000 | 0.011** |
| Banyoles and EMH | 0.04 | −8.31 | 0.003 | <0.001*** | 10000 | 0.002*** |
| Banyoles and NT | 0.07 | 13.17 | 0.003 | <0.001*** | 10000 | <0.001*** |
| Banyoles and MPE | 0.08 | 18.92 | 0.003 | <0.001*** | 10000 | <0.001*** |

Abbreviations: RMH = Recent Modern Human, UPMH = Upper Paleolithic Modern Human, EMH = Early Modern Human, NT = Neandertal, MPE = Middle Pleistocene European.
[a] * = $p < 0.05$; ** = $p < 0.01$; *** = $p < 0.001$.

**Table 13**
Results of permuted Canonical Variate Analysis (CVA) to test whether the Procrustes distances of each group to the reconstructions of Banyoles are statistically different.

| Groups compared | Procrustes distance | Permutations | Permutated *p*-value[a] |
|---|---|---|---|
| Banyoles and RMH | 0.0925 | 10000 | <0.001*** |
| Banyoles and UPMH | 0.0878 | 10000 | 0.005** |
| Banyoles and EMH | 0.1100 | 10000 | 0.043* |
| Banyoles and NT | 0.1209 | 10000 | 0.028* |
| Banyoles and MPE | 0.1305 | 10000 | 0.029* |

Abbreviations: RMH = Recent Modern Human, UPMH = Upper Paleolithic Modern Human, EMH = Early Modern Human, NT = Neandertal, MPE = Middle Pleistocene European.
[a] * = $p < 0.05$; ** = $p < 0.01$; *** = $p < 0.001$.

features in Banyoles clearly differentiates this specimen from Neandertals but resembles non-Neandertal archaic *Homo* mandibles from Africa and Asia and *H. sapiens* more closely. Nevertheless, most of the features in *H. sapiens* mandibles seem to be largely primitive retentions, making them less useful in taxonomic diagnoses in individual specimens. While the expression for some of the features in Banyoles (e.g., more anterior placement of the mental foramen or absence of the medial pterygoid tubercle) can occasionally be found in Neandertals (Franciscus and Trinkaus, 1995; Bermúdez de Castro et al., 2015), the expanded gonial margin differentiates Banyoles from European Middle Pleistocene specimens and Neandertals.

Given its chronological and geographic context in Upper Pleistocene Western Europe, the most relevant comparisons for Banyoles are with Neandertals and *H. sapiens*. Importantly, several of the morphological features analyzed are argued to show a derived expression in Neandertals, including the posterior position of the mental foramen, typically below the $M_1$, the presence of a retromolar space behind the $M_3$, the high placement of the mylohyoid line at the $M_3$ and its steep inclination anteriorly, a truncated and inverted gonial margin, and the presence of a medial pterygoid tubercle and H-O mandibular foramen on the medial ramus. Unfortunately, damage to Banyoles precludes assessment of the superior ramus anatomy, a region that has been shown to be highly derived in Neandertals (Rak et al., 2002). Nevertheless, the expression of all the morphological features in Banyoles differs from that seen in Neandertals, and Banyoles appears not to show any clearly derived Neandertal mandibular features.

The single uniquely derived feature in the *H. sapiens* mandible is the presence of a bony chin. While individual elements of the *H. sapiens* chin can occasionally be found in Neandertals (e.g., Quam et al., 2001, 2011) and other early *Homo* specimens (e.g., UR 501, OH 7, OH 13, KNM-ER 730, Dmanisi, D211 and D2735, ATE9-1, or Sangiran 9 and 22), the full combination of features that comprise the *H. sapiens* chin are found exclusively in *H. sapiens* (Schwartz and Tattersall, 2000). Notably, most of these features are absent in Banyoles. While the symphysis is essentially vertical, and not retreating, the external symphyseal face shows at most a minimal expression of chin features. However, one potential explanation for Banyoles' unexpected symphyseal morphology may be related to the severe anterior dental wear.

Banyoles thus lacks any derived Neandertal or *H. sapiens* features. Rather, the morphology of Banyoles seems to be that of a generalized, primitive form of the genus *Homo*, despite its relatively late chronology and its geographic location in Western Europe. Despite a lack of clearly derived morphological features, the 3D GM analysis grouped Banyoles with *H. sapiens* in the overall shape of the mandible, and the closest specimens to Banyoles are recent and fossil *H. sapiens* individuals. Given the considerable degree of overlap between groups along PC1, this result was largely driven by its placement along PC2, and reflects the expanded gonial region, vertical symphysis, narrower ramus width, more anterior mental foramen position, and shorter dental arcade in Banyoles. The two non-*H. sapiens* fossils that fell closest to Banyoles along PC2 are La Quina H5 and Tighenif 3, but these aspects of Banyoles generally differentiate the specimen from Middle Pleistocene specimens and Neandertals.

Furthermore, the allometric signal for PC2 is interesting, especially considering that negative PC2 scores indicate a more posterior position of the mental foramen and also a retreating symphyseal region (see below), which has been found to be positively allometric by Rosas and Bastir (2004). This study thus supports the allometric significance of these features in mandibular variation. However, while PC2 may show a significant allometric effect overall, the total shape variances across all PC axes computed in this study show a biological signal that cannot be fully explained by size-correlated shape change.

### 4.1. Taxonomic considerations for Banyoles

Numerous researchers have suggested affinities for Banyoles with the Neandertals or MPE specimens (Hernandez-Pacheco and Obermaier, 1915; Bonarelli, 1916; Sergi, 1917; Keith, 1931; Hoyos-Sáinz, 1947; de Lumley, 1971–1972; Roth, 1982; Sánchez-Lopez, 1993; Roth et al., 1993; Rosas, 1993). However, given the Late Pleistocene age of Banyoles and its generalized morphology, other interpretations should be considered (Table 14).

One possibility is that the specimen represents a late-surviving individual of a Middle Pleistocene population. In Europe, there appear broadly to be two Middle Pleistocene hominin populations (Tattersall, 2011). One is represented by fossils that show clearly derived Neandertal features, like those from the sites of the Sima de los Huesos, Payre, Ehringsdorf and l'Aubesier (Arsuaga et al., 2014). The other generally seems to lack derived Neandertal features, as represented most clearly by Mala Balanica, Mauer, and Ceprano, although the latter lacks an associated mandible (Manzi et al., 2001; Rak et al., 2002; Roksandic et al., 2011). However, these latter fossils all pre-date Banyoles by at least 300 kyr, based on the date for Ceprano (Muttoni et al., 2009), the youngest specimen among them, and all MPE mandibles younger than the Ceprano cranium show derived Neandertal features (e.g., Ehringsdorf, La Chaise-BD, Payre; Vlcek, 1993; Condemi, 2001; Verna et al., 2020). This makes it unlikely that Banyoles represents a late-surviving individual of this non-Neandertal European group.

Middle Pleistocene fossils that appear to lack clear Neandertal affinities have also been reported from some sites in the Middle East, including Zuttiyeh and (perhaps) Qesem (Hershkovitz et al., 2011; Freidline et al., 2012). Nevertheless, no mandible is preserved at either of these sites, complicating a direct comparison with Banyoles. In contrast, the recently discovered mandible from the site of Nesher Ramla dates to ca. 140 ka and shows some Neandertal affinities (Hershkovitz et al., 2021; Marom and Rak, 2021; May et al., 2021). Nesher Ramla is similar to Banyoles in

**Table 14**
Taxonomic considerations for Banyoles.

| Group | Not possible | Unlikely | Possible | Reason |
|---|---|---|---|---|
| European Middle Pleistocene specimen | X | | | Late Pleistocene date |
| Late-surviving European Middle Pleistocene specimen | | X | | Middle Pleistocene fossils <400 kya all show Neandertal features |
| Late-surviving Levantine Middle Pleistocene specimen | | X | | No clear affinities with Nesher Ramla |
| Neandertal | X | | | No Neandertal features present |
| Neandertal/*Homo sapiens* hybrid | X | | | No Neandertal features present |
| *Homo sapiens* | | | X | 3D GM placement |
| Non-Neandertal/*Homo sapiens* hybrid | | | X | 3D GM placement and rudimentary chin structures |

the details of the anterior symphyseal morphology (i.e., lack of chin structures), in showing parallel alveolar and basal borders of the corpus, and in the lack of both an H-O mandibular foramen and bridging of the mylohyoid line. Nesher Ramla differs from Banyoles in showing a more posteriorly placed mental foramen, a likely retromolar space behind the $M_3$, a more steeply inclined mylohyoid line and inferiorly facing digastric fossae. Thus, Neandertal affinities are more clearly expressed in Nesher Ramla than in Banyoles. The 3D GM analysis in the Nesher Ramla study also included Banyoles in the comparative sample, but these two specimens did not cluster closely together in shape space (Hershkovitz et al., 2021). Rather, Nesher Ramla fell closest to the Neandertals, while Banyoles fell closest to the *H. sapiens* specimens in the analysis (Hershkovitz et al., 2021). This makes it unlikely that Banyoles represents a late-surviving individual of this Levantine Middle Pleistocene group.

The lack of Neandertal features and the Upper Pleistocene age of Banyoles suggest a possible assignment to *H. sapiens*, despite the lack of chin structures. In fact, the expression of chin features is somewhat attenuated in fossils that have been attributed to early *H. sapiens*. The juvenile mandible Jebel Irhoud 3 shows a raised central keel and mental fossae on either side of the midline and an inferiorly positioned mental trigone (Hublin and Tillier, 1981; Hublin et al., 2017). These same features are less pronounced in the adult Jebel Irhoud 11 mandible which, however, does show some curvature of the anterior face (incurvatio mandibulae anterior; Hublin et al., 2017). Jebel Irhoud 11 is similar to the Tabun C2 mandible in a number of details, including the symphyseal morphology. In particular, Tabun C2 shows a clear depression below the incisors (incurvatio mandibulae anterior) and some development of pogonion, and this specimen has been argued to show modern affinities (Quam and Smith, 2002).

Similarly, the early *H. sapiens* specimens from Qafzeh and Skhul show variable development of the chin structures, with several specimens showing a broad depression just below the incisors and a swelling at the base of the anterior symphysis but lacking a central keel and well-defined mental trigone (Schwartz and Tattersall, 2000). Thus, early *H. sapiens* fossils show incomplete and variable development of the chin structures, although all these specimens predate Banyoles by at least 30 ka (Skhul/Qafzeh) and as much as 200 ka (Hublin et al., 2017).

Fossils attributed to *H. sapiens* that are approximately contemporaneous with Banyoles (ca. 45–66 ka) have recently been documented at the Grotte Mandrin in France (ca. 51.7–56.8 ka; Slimak et al., 2022) and at the Levantine site of Manot (ca. 66 ka; Alex et al., 2017). Unfortunately, no mandible is preserved at either of these sites, so it is not possible to draw any conclusions regarding affinities with Banyoles. Other European sites that have yielded *H. sapiens* fossils that may overlap chronologically with Banyoles include Bacho Kiro, Peştera cu Oase, Zlatý Kůň, and Kent's Cavern. Of these specimens, the Oase 1 mandible provides the most direct comparison with Banyoles. Notably, both Banyoles and Oase 1 show an expanded gonial profile and vertical symphysis, features which distinguish them from Neandertals. However, Oase 1 differs from Banyoles in showing a clear H-O form of the mandibular foramen on one side, a very wide ramus and a greater development of the chin structures, including the presence of a prominent symphyseal tubercle and lateral fossae, and a mentum osseum rank of 4 (Trinkaus and Rougier, 2013). Notably, ancient DNA evidence for Oase 1 revealed that this specimen shared 6–9% of its DNA with Neandertals and may have had a Neandertal ancestor as recently as 4–6 generations ago (Fu et al., 2015).

Ancient DNA sequencing of the Neandertal genome within the last decade has shed light on our understanding of Neandertal and *H. sapiens* admixture (Green et al., 2010; Sánchez-Quinto et al., 2012; Sankararaman et al., 2012; Prüfer et al., 2014; Fu et al., 2014, 2015; Posth et al., 2017). Prüfer et al. (2014) found that RMH shares on average 1.4–2.1% of Neandertal DNA based on a complete genome sequence from the Neandertal found in the Altai mountains. That same year Lohse and Frantz (2014) compared three RMH genomes to that of a Neandertal from the site of Vindija (Croatia) and found even higher shared DNA ranging from 3.4 to 7.9%.

These genetic studies also shed light on the timing of Neandertal and RMH admixture. More recently, Posth et al. (2017) proposed genetic evidence for an early, and potentially ancestral, African population introgression event before 270 ka in the Neandertal lineage to explain a discrepancy in the mitochondrial genome of Neandertals from their genetic predecessors. Another study by Sankararaman et al. (2012) demonstrated that the latest episode of gene flow from Neandertals to non-Africans most likely occurred between 47 and 65 ka. Based on the fossil genetic evidence, one of the earliest *H. sapiens* in Europe, Peştera cu Oase 1, was found to share 6–9% Neandertal DNA. Mitochondrial DNA of *H. sapiens* was sequenced from bone fragments at Bacho Kiro Cave, Bulgaria dating to 46 ka but found no evidence of Neandertal admixture (Hublin et al., 2020). In Western Siberia, the Ust-Ishim *H. sapiens* dating to 45 ka was found to share 2.3% Neandertal DNA (Fu et al., 2014). In Czechia, the Zlatý Kůň cranium dated to a minimum of 45 ka was found to share around 3% Neandertal DNA (Prüfer et al., 2021). Also, in the Middle East, where the oldest *H. sapiens* fossils are found outside of Africa, Green et al. (2010) hint at a single admixture event occurring there and suggest it fits a timeline of 50–80 ka (Green et al., 2010; Smith, 2013; Wall et al., 2013). Thus, while Neandertals disappeared from the fossil record as a distinct biological entity during the second half of the Late Pleistocene, genetic admixture with *H. sapiens* occurred on more than one occasion, and their genetic legacy lives on today in RMH.

Furthermore, several studies on hybridity in the genus *Homo* (Duarte et al., 1999; Tattersall and Schwartz, 1999; Trinkaus et al., 2003; Gunz and Harvati, 2011; Smith, 2013; Ackermann et al., 2016; Smith et al., 2017) have argued for species/subspecies introgression by highlighting a derived feature of one species in an individual of another separate species/subspecies, and the mixture of Neandertal and *H. sapiens* features in Oase 1 is consistent with this perspective. In contrast, the lack of Neandertal features in Banyoles would seem to rule out hybridization with a Neandertal, but admixture with a non-Neandertal archaic *Homo* ancestor could still potentially account for why Banyoles retained primitive features not seen in modern *H. sapiens*. Notably, some attenuated chin structures have been argued to be present in both the Zhoukoudian and Tighenif mandibles (Weidenreich, 1936; Schwartz and Tattersall, 2000), although both samples are far removed from Banyoles in time and geography, making these populations unlikely candidates for hybridization or gene flow with Banyoles. While the lack of chin structures in Banyoles might be explained by admixture with a non-Neandertal archaic *Homo* form, no such population has been identified in the Late Pleistocene European fossil record.

## 5. Conclusions

The results of the present study have demonstrated clearly that Banyoles does not show any derived Neandertal features. This calls into question previous assessments of Banyoles as representing either a Neandertal or a Middle Pleistocene Neandertal precursor. While the precise taxonomic classification is uncertain, Banyoles clearly does not represent a Neandertal. The age range for Banyoles is approximately 45–66 ka and broadly corresponds to when Neandertals were present throughout Europe. Thus, the lack of Neandertal features in Banyoles is surprising. The age range of

Banyoles does also encompass the date for early *H. sapiens* fossils from the Levant and Europe.

Thus, this study argues Banyoles represents a non-Neandertal Late Pleistocene European individual. The 3D GM analysis clearly grouped Banyoles with *H. sapiens*, but the lack of chin structures complicates this assignment and leaves a taxonomic decision on the specimen currently open. While the lack of chin structures in Banyoles might be explained by admixture with a non-Neandertal archaic *Homo* form, no such population has been identified in the Late Pleistocene European fossil record, and European Middle Pleistocene fossils that lack Neandertal features predate Banyoles by at least 300 ka. The present situation makes Banyoles a prime candidate for ancient DNA or proteomic analyses, which may shed additional light on its taxonomic affinities. Regardless, Banyoles highlights the continuing signal of diversity in the human fossil record.

## Data availability

The CT scan of the Banyoles mandible used in this study is available for download from www.morphosource.org.

## Declaration of competing interest

The authors declare to have no competing interests.

## Acknowledgments

We would like to express our gratitude to the Alsius family for giving us permission to study the Banyoles mandible and for providing us access to the CT scan to conduct this study. Special thanks to Ana Pantoja for her helpful advice on virtual reconstruction. We also would like to thank the family for allowing us to upload the CT scan and 3D model of the Banyoles mandible used in this study to the digital skeletal repository Morphosource.org. Thank you very much Gisselle Garcia, Ian Tattersall, and Will Harcourt-Smith at the American Museum of Natural History, New York, for access to the comparative specimens and scanning equipment. We would also like to express our gratitude for $\mu$CT scans of fossils from Tel Aviv University (I. Hershkovitz and J. Abramov) and the Museé de l'Homme (A. Balzeau) in Paris. Thank you to Soprintendenza Archeologia, Belle Arti e Paesaggio per l'area Metropolitana di Roma e per la Provincia di Rieti (N. Radi and V. Sparacello) for access to the Arene Candide mandibles compared in this study. Finally, thank you to the editors and two anonymous reviewers for their advice and helpful suggestions. This study forms part of Project PID2021-122355NB-C31 supported by MCIN/AEI/10.13039/501100011033/FEDER, UE of the Government of Spain.

## Supplementary Online Material

Supplementary online material related to this article can be found at https://doi.org/10.1016/j.jhevol.2022.103291.

## References

Ackermann, R.R., Mackay, A., Arnold, M.L., 2016. The hybrid origin of “modern” humans. Evol. Biol. 43, 1–11.
Adams, D.C., Otárola-Castillo, E., 2013. Geomorph: An r package for the collection and analysis of geometric morphometric shape data. Methods Ecol. Evol. 4, 393–399.
Ahern, J.C.M., Janković, I., Voisin, J.-L., Smith, F.H., 2013. Modern human origins in Central Europe. In: Smith, F.H., Ahern, J.C.M. (Eds.), The Origins of Modern Humans. John Wiley & Sons, Inc., Hoboken, pp. 151–221.
Alcázar de Velasco, A., Arsuaga, J.L., Martínez Mendizábal, I., Bonmatí, A., 2011. Revisión de la mandíbula humana de Bañolas, Gerona, España. Bol. R. Soc. Esp. Hist. Nat. Sec. Geol. 105, 99–108.
Alcobé, S., 1993. Mandibula de Banyoles, diario de trabajo. In: Maroto, J. (Ed.), La Mandíbula de Banyoles En El Context Dels Fòssils Humans Del Pleistocè, Centre d'Investigacions Arqueològiques Gerona: Serie Monográfica. Centre d'Investigacions Arqueològiques de Girona, Girona, pp. 59–66.
Alex, B., Barzilai, O., Hershkovitz, I., Marder, O., Berna, F., Caracuta, V., Abulafia, T., Davis, L., Goder-Goldberger, M., Lavi, R., Mintz, E., Regev, L., Bar-Yosef Mayer, D., Tejero, J.-M., Yeshurun, R., Ayalon, A., Bar-Matthews, M., Yasur, G., Frumkin, A., Latimer, B., Hans, M.G., Boaretto, E., 2017. Radiocarbon chronology of Manot Cave, Israel and Upper Paleolithic dispersals. Sci. Adv. 3, e1701450.
Alsius, P., 1907. El Magdalenense en la Provincia de Gerona. Documenta Universitaria, Banyoles.
Alsius, P., 1915. De la barra humana descoberta anys enrera a Banyoles. Institucio Catalana D' Historia Natural, pp. 126–131.
Arsuaga, J.L., Martínez, I., Arnold, L.J., Aranburu, A., Gracia-Téllez, A., Sharp, W.D., Quam, R.M., Falguères, C., Pantoja-Pérez, A., Bischoff, J., Poza-Rey, E., Parés, J.M., Carretero, J.M., Demuro, M., Lorenzo, C., Sala, N., Martinón-Torres, M., García, N., Alcázar de Velasco, A., Cuenca-Bescós, G., Gómez-Olivencia, A., Moreno, D., Pablos, A., Shen, C.-C., Rodríguez, L., Ortega, A.I., García, R., Bonmatí, A., Bermúdez de Castro, J.M., Carbonell, E., 2014. Neandertal roots: Cranial and chronological evidence from Sima de los Huesos. Science 344, 1358–1363.
Baken, E.K., Collyer, M.L., Kaliontzopoulou, A., Adams, D.C., 2021. geomorph v4.0 and gmShiny: Enhanced analytics and a new graphical interface for a comprehensive morphometric experience. Methods Ecol. Evol. 12, 2355–2363.
Bech, J., 1971. Contribution a la connaissance de la chronologie des terrasses lacustres de Banyoles (Gerona). Quaternaire 8, 15–20.
Been, E., Hovers, E., Ekshtain, R., Malinski-Buller, A., Agha, N., Barash, A., Mayer, D.E.B.-Y., Benazzi, S., Hublin, J.-J., Levin, L., Greenbaum, N., Mitki, N., Oxilia, G., Porat, N., Roskin, J., Soudack, M., Yeshurun, R., Shahack-Gross, R., Nir, N., Stahlschmidt, M.C., Rak, Y., Barzilai, O., 2017. The first Neanderthal remains from an open-air Middle Palaeolithic site in the Levant. Sci. Rep. 7, 2958.
Benazzi, S., Stansfield, E., Kullmer, O., Fiorenza, L., Gruppioni, G., 2009. Geometric morphometric methods for bone reconstruction: The mandibular condylar process of Pico della Mirandola. Anat. Rec. 292, 1088–1097.
Benazzi, S., Douka, K., Fornai, C., Bauer, C.C., Kullmer, O., Svoboda, J., Pap, I., Mallegni, F., Bayle, P., Coquerelle, M., Condemi, S., Ronchitelli, A., Harvati, K., Weber, G.W., 2011. Early dispersal of modern humans in Europe and implications for Neanderthal behaviour. Nature 479, 525–528.
Berger, R., Libby, W.F., 1966. UCLA radiocarbon dates V. Radiocarbon 8, 467–497.
Bermúdez de Castro, J.-M., Martinón-Torres, M., Gómez-Robles, A., Prado, L., Sarmiento, S., 2007. Comparative analysis of the Gran Dolina-TD6 (Spain) and Tighennif (Algeria) hominin mandibles. Bull. Mem. Soc. Anthropol. Paris 19, 149–167.
Bermúdez de Castro, J.M., Martinón-Torres, M., Gómez-Robles, A., Prado, L., Carbonell, E., 2010. New human evidence of the Early Pleistocene settlement of Europe, from Sima del Elefante site (Sierra de Atapuerca, Burgos, Spain). Quat. Int. 223–224, 431–433.
Bermúdez de Castro, J.-M., Quam, R., Martinón-Torres, M., Martínez, I., Gracia-Téllez, A., Arsuaga, J.L., Carbonell, E., 2015. The medial pterygoid tubercle in the Atapuerca Early and Middle Pleistocene mandibles: Evolutionary implications: Medial pterygoid tubercle in Atapuerca. Am. J. Phys. Anthropol. 156, 102–109.
Bonarelli, G., 1916. La mandibula humana de Bañolas. Physis 2, 399–406.
Broca, P., 1868. Sur les crânes et ossements des Eyzies. Bull. Mem. Soc. Anthropol. Paris 3, 350–392.
Buikstra, J.E., Ubelaker, D.H. (Eds.), 1994. Standards for data collection from human skeletal remains. Arkansas Archaeological Survey Research Series, vol. 44. Fayetteville.
Busk, G., 1865. On a very ancient human cranium from Gibraltar. Rep. Br. Assoc. Adv. Sci. Bath. 1864, 91–92.
Carbonell, E., Bermúdez de Castro, J.M., Arsuaga, J.L., Allue, E., Bastir, M., Benito, A., Cáceres, I., Canals, T., Díez, J.C., van der Made, J., Mosquera, M., Ollé, A., Pérez-González, A., Rodríguez, J., Rodríguez, X.P., Rosas, A., Rosell, J., Sala, R., Vallverdú, J., Vergés, J.M., 2005. An Early Pleistocene hominin mandible from Atapuerca-TD6, Spain. Proc. Natl. Acad. Sci. USA 102, 5674–5678.
Carbonell, E., Bermúdez de Castro, J.M., Parés, J.M., Pérez-González, A., Cuenca-Bescós, G., Ollé, A., Mosquera, M., Huguet, R., van der Made, J., Rosas, A., Sala, R., Vallverdú, J., García, N., Granger, D.E., Martinón-Torres, M., Rodríguez, X.P., Stock, G.M., Vergès, J.M., Allué, E., Burjachs, F., Cáceres, I., Canals, A., Benito, A., Díez, C., Lozano, M., Mateos, A., Navazo, M., Rodríguez, J., Rosell, J., Arsuaga, J.L., 2008. The first hominin of Europe. Nature 452, 465–469.
Condemi, S., 2001. Les Néandertaliens de La Chaise: Abri Bourgeois-Delaunay. Comité des travaux historiques et scientifiques-CTHS, Aubervilliers.
Creed-Miles, M., Rosas, A., Kruszynski, R., 1996. Issues in the identification of Neandertal derivative traits at early post-natal stages. J. Hum. Evol. 30, 147–153.
Daegling, D.J., 2005. Functional morphology of the human chin. J. Hum. Evol. 1, 170–177.
Daura, J., Sanz, M., Subirá, M., Quam, R., Fullola, J., Arsuaga, J., 2005. A Neandertal mandible from the Cova del Gegant (Sitges, Barcelona, Spain). J. Hum. Evol. 49, 56–70.
de Lumley, M.A., 1971–1972. La mandíbula de Bañolas. Ampurias: Revista de arqueología, prehistoria y etnografía 33, 1–92.
de Lumley, M.A., 1973. Anteneándertaliens et Néandertaliens du bassin méditerranéen occidental européen: Cova Negra, Le Lazaret, Bañolas, Grotte de Prince, Carigüela, Hortus, Agut, Macassargues, La Masque, Rigabe, La Crouzade, Les Peyrads, Bau de l'Aubesier. Université de Provence, Marseille.
de Lumley, M.A., 1993. Antecedents i problematica de l'estudi de la mandíbula de Banyoles. In: Maroto, J. (Ed.), La Mandíbula de Banyoles En El Context Dels

Fòssils Humans Del Pleistocè. Centre d'investigacions arqueològiques sèrie monogràfica, Girona, Spain, pp. 35–54.
De-Ary-Pires, B., Ary-Pires, R., Pires-Neto, M.A., 2003. The human digastric muscle: Patterns and variations with clinical and surgical correlations. Ann. Anat. 185, 471–479.
Delacre, M., Lakens, D., Leys, C., 2017. Why psychologists should by default use Welch's t-test instead of Student's t-test. Int. Rev. Soc. Psychol. 30, 92.
Dobson, S.D., Trinkaus, E., 2002. Cross-sectional geometry and morphology of the mandibular symphysis in Middle and Late Pleistocene *Homo*. J. Hum. Evol. 43, 67–87.
Duarte, C., Maurício, J., Pettitt, P.B., Souto, P., Trinkaus, E., Van Der Plicht, H., Zilhão, J., 1999. The early Upper Paleolithic human skeleton from the Abrigo do Lagar Velho (Portugal) and modern human emergence in Iberia. Proc. Natl. Acad. Sci. USA 96, 7604–7609.
Fraipont, J., Lohest, M., 1887. La race humaine de Néanderthal ou de Canstadt en Belgique: Recherches ethnographiques sur des ossements humains découvert dans les depôts quaternaires d'une grotte à Spy et détermination de leur âge géologique. Extrait des Archives de Biologie. In: Éd Van Beneden, M.M., Van Bambeke, C.H. (Eds.), Tome VII, Vanderpoorten, Ghent.
Franciscus, R.G., Trinkaus, E., 1995. Determinants of retromolar space presence in Pleistocene *Homo* mandibles. J. Hum. Evol. 28, 577–595.
Freidline, S.E., Gunz, P., Janković, I., Harvati, K., Hublin, J.J., 2012. A comprehensive morphometric analysis of the frontal and zygomatic bone of the Zuttiyeh fossil from Israel. J. Hum. Evol. 62, 225–241.
Fu, Q., Li, H., Moorjani, P., Jay, F., Slepchenko, S.M., Bondarev, A.A., Johnson, P.L.F., Aximu-Petri, A., Prüfer, K., de Filippo, C., Meyer, M., Zwyns, N., Salazar-García, D.C., Kuzmin, Y.V., Keates, S.G., Kosintsev, P.A., Razhev, D.I., Richards, M.P., Peristov, N.V., Lachmann, M., Douka, K., Higham, T.F.G., Slatkin, M., Hublin, J.-J., Reich, D., Kelso, J., Viola, T.B., Pääbo, S., 2014. Genome sequence of a 45,000-year-old modern human from western Siberia. Nature 514, 445–449.
Fu, Q., Hajdinjak, M., Moldovan, O.T., Constantin, S., Mallick, S., Skoglund, P., Patterson, N., Rohland, N., Lazaridis, I., Nickel, B., Viola, B., Prüfer, K., Meyer, M., Kelso, J., Reich, D., Pääbo, S., 2015. An early modern human from Romania with a recent Neanderthal ancestor. Nature 524, 216–219.
Garnier, S., 2021. swaRm: a package For processing collective movement data. https://swarm-lab.github.io/swaRm/.
Giuffrida-Ruggeri, 1921. Su l'origine dell'uomo: Nuove teorie e documenti; con 24 figure. Zanichelli, Bologna.
Green, R.E., Krause, J., Briggs, A.W., Maricic, T., Stenzel, U., Kircher, M., Patterson, N., Li, H., Zhai, W., Fritz, M.H.-Y., Hansen, N.F., Durand, E.Y., Malaspinas, A.-S., Jensen, J.D., Marques-Bonet, T., Alkan, C., Prüfer, K., Meyer, M., Burbano, H.A., Good, J.M., Schultz, R., Aximu-Petri, A., Butthof, A., Höber, B., Höffner, B., Siegemund, M., Weihmann, A., Nusbaum, C., Lander, E.S., Russ, C., Novod, N., Affourtit, J., Egholm, M., Verna, C., Rudan, P., Brajkovic, D., Kucan, Ž., Gušic, I., Doronichev, V.B., Golovanova, L.V., Lalueza-Fox, C., de la Rasilla, M., Fortea, J., Rosas, A., Schmitz, R.W., Johnson, P.L.F., Eichler, E.E., Falush, D., Birney, E., Mullikin, J.C., Slatkin, M., Nielsen, R., Kelso, J., Lachmann, M., Reich, D., Pääbo, S., 2010. A draft sequence of the Neandertal genome. Science 328, 710–722.
Grün, R., Maroto, J., Eggins, S., Stringer, C., Robertson, S., Taylor, L., Mortimer, G., McCulloch, M., 2006. ESR and U-series analyses of enamel and dentine fragments of the Banyoles mandible. J. Hum. Evol. 50, 347–358.
Gunz, P., Harvati, K., 2011. Integration and homology of "chignon" and "hemibun" morphology. In: Condemi, S., Weniger, G.C. (Eds.), Continuity and Discontinuity in the Peopling of Europe. Springer Netherlands, Dordrecht, pp. 193–202.
Harvati, K., Röding, C., Bosman, A.M., Karakostis, F.A., Grün, R., Stringer, C., Karkanas, P., Thompson, N.C., Koutoulidis, V., Moulopoulos, L.A., 2019. Apidima Cave fossils provide earliest evidence of *Homo sapiens* in Eurasia. Nature 571, 500–504.
Hernandez-Pacheco, E., Obermaier, H., 1915. La mandíbula Neandertaloide de Bañolas, Comision de Investigaciones Paleontoogicas Y Prehistoricas. Comision de Investigaciones Paleontoogicas Y Prehistoricas, Madrid, Spain.
Hershkovitz, I., Smith, P., Sarig, R., Quam, R., Rodríguez, L., García, R., Arsuaga, J.L., Barkai, R., Gopher, A., 2011. Middle Pleistocene dental remains from Qesem Cave (Israel). Am. J. Phys. Anthropol. 144, 575–592.
Hershkovitz, I., Marder, O., Ayalon, A., Bar-Matthews, M., Yasur, G., Boaretto, E., Caracuta, V., Alex, B., Frumkin, A., Goder-Goldberger, M., Gunz, P., Holloway, R.L., Latimer, B., Lavi, R., Matthews, A., Slon, V., Mayer, D.B.-Y., Berna, F., Bar-Oz, G., Yeshurun, R., May, H., Hans, M.G., Weber, G.W., Barzilai, O., 2015. Levantine cranium from Manot Cave (Israel) foreshadows the first European modern humans. Nature 520, 216–219.
Hershkovitz, I., May, H., Sarig, R., Pokhojaev, A., Grimaud-Hervé, D., Bruner, E., Fornai, C., Quam, R., Arsuaga, J.L., Krenn, V.A., Martinón-Torres, M., de Castro, J.M.B., Martín-Francés, L., Slon, V., Albessard-Ball, L., Vialet, A., Schüler, T., Manzi, G., Profico, A., Di Vincenzo, F., Weber, G.W., Zaidner, Y., 2021. A Middle Pleistocene *Homo* from Nesher Ramla, Israel. Science 372, 1424–1428.
Higham, T., Compton, T., Stringer, C., Jacobi, R., Shapiro, B., Trinkaus, E., Chandler, B., Gröning, F., Collins, C., Hillson, S., O'Higgins, P., FitzGerald, C., Fagan, M., 2011. The earliest evidence for anatomically modern humans in northwestern Europe. Nature 479, 521–524.
Higham, T., Douka, K., Wood, R., Ramsey, C.B., Brock, F., Basell, L., Camps, M., Arrizabalaga, A., Baena, J., Barroso-Ruíz, C., Bergman, C., Boitard, C., Boscato, P., Caparrós, M., Conard, N.J., Draily, C., Froment, A., Galván, B., Gambassini, P., Garcia-Moreno, A., Grimaldi, S., Haesaerts, P., Holt, B., Iriarte-Chiapusso, M.-J., Jelinek, A., Jordá Pardo, J.F., Maíllo-Fernández, J.-M., Marom, A., Maroto, J., Menéndez, M., Metz, L., Morin, E., Moroni, A., Negrino, F., Panagopoulou, E., Peresani, M., Pirson, S., de la Rasilla, M., Riel-Salvatore, J., Ronchitelli, A., Santamaria, D., Semal, P., Slimak, L., Soler, J., Soler, N., Villaluenga, A., Pinhasi, R., Jacobi, R., 2014. The timing and spatiotemporal patterning of Neanderthal disappearance. Nature 512, 306–309.
Hoyos-Sáinz, L., 1947. Antropologia prehistórica espanola. In: Menendez Pidal, R. (Ed.), Historia de España. Espasa-Calpe, Madrid, pp. 95–241.
Hublin, J.J., Tillier, A.M., 1981. The Mousterian juvenile mandible from Irhoud (Morocco): A phylogenetic interpretation. In: Stringer, C.B. (Ed.), Aspects of Human Evolution. Taylor and Francis, London, pp. 167–185.
Hublin, J.-J., Ben-Ncer, A., Bailey, S.E., Freidline, S.E., Neubauer, S., Skinner, M.M., Bergmann, I., Le Cabec, A., Benazzi, S., Harvati, K., Gunz, P., 2017. New fossils from Jebel Irhoud, Morocco and the Pan-African origin of *Homo sapiens*. Nature 546, 289–292.
Hublin, J.-J., Sirakov, N., Aldeias, V., Bailey, S., Bard, E., Delvigne, V., Endarova, E., Fagault, Y., Fewlass, H., Hajdinjak, M., Kromer, B., Krumov, I., Marreiros, J., Martisius, N.L., Paskulin, L., Sinet-Mathiot, V., Meyer, M., Pääbo, S., Popov, V., Rezek, Z., Sirakova, S., Skinner, M.M., Smith, G.M., Spasov, R., Talamo, S., Tuna, T., Wacker, L., Welker, F., Wilcke, A., Zahariev, N., McPherron, S.P., Tsanova, T., 2020. Initial Upper Palaeolithic *Homo sapiens* from Bacho Kiro Cave, Bulgaria. Nature 581, 299–302.
Jidoi, K., Nara, T., Dodo, Y., 2000. Bony bridging of the mylohyoid groove of the human mandible. Anthropol. Sci. 108, 345–370.
Julià, R., Bischoff, J.L., 1991. Radiometric dating of quaternary deposits and the hominid mandible of lake Banyolas, Spain. J. Archaeol. Sci. 18, 707–722.
Julià, R., Maroto, J., Narcís, S., 1987. La mandíbula de Banyoles. Antecedents i context de la seva troballa. Cypsela VI, 43–52.
Keith, A., 1931. New Discoveries Relating to the Antiquity of Man. Williams & Norgate, Ltd., London Press, London.
Klingenberg, C.P., 2011. MorphoJ: An integrated software package for geometric morphometrics: Computer program note. Mol. Ecol. Res. 11, 353–357.
Kohl, M., 2020. MKinfer: Inferential Statistics. https://cran.r-project.org/web/packages/MKinfer/index.html.
Lalueza, C., Pérez-Pérez, A., Turbón, D., 1993. Microscopic study of the Banyoles mandible (Girona, Spain): Diet, cultural activity and toothpick use. J. Hum. Evol. 24, 281–300.
Lipski, M., Tomaszewska, I.M., Lipska, W., Lis, G.J., Tomaszewski, K.A., 2013. The mandible and its foramen: Anatomy, anthropology, embryology and resulting clinical implications. Folia Morphol. 72, 285–292.
Liu, W., Jin, C.-Z., Zhang, Y.-Q., Cai, Y.-J., Xing, S., Wu, X.-J., Cheng, H., Edwards, R.L., Pan, W.-S., Qin, D.-G., An, Z.-S., Trinkaus, E., Wu, X.-Z., 2010. Human remains from Zhirendong, South China, and modern human emergence in East Asia. Proc. Natl. Acad. Sci. USA 107, 19201–19206.
Lohse, K., Frantz, L.A.F., 2014. Neandertal admixture in Eurasia confirmed by maximum-likelihood analysis of three genomes. Genetics 196, 1241–1251.
MacCurdy, G.G., 1915. Neandertal man in Spain: The lower jaw of Bañolas. Science 42, 84–85.
Manzi, G., Mallegni, F., Ascenzi, A., 2001. A cranium for the earliest Europeans: Phylogenetic position of the hominid from Ceprano, Italy. Proc. Natl. Acad. Sci. USA 98, 10011–10016.
Marom, A., Rak, Y., 2021. Comment on "A Middle Pleistocene *Homo* from Nesher Ramla, Israel.". Science 374, eabl4336.
Maroto, J., 1987. La mandibula de Banyoles, un descobriment centenari. Rev. Girona 122, 82–86.
Maroto, J., 1993. La mandíbula de Banyoles en el context dels fòssils humans del Pleistocè. Centre D'investigacions Arqueològiques Sèrie Monogràfica, Girona.
Maroto, J., Soler, N., 1993. Antecedents i problemática de l'estudi de la mandíbula de Banyoles. In: Maroto, J. (Ed.), La Mandíbula de Banyoles En El Context Dels Fòssils Humans Del Pleistocene. Centre D'Investigacions Arqueològiques Sèrie Monogràfica, Girona, pp. 35–54.
May, H., Sarig, R., Pokhojaev, A., Fornai, C., Martinón-Torres, M., Bermúdez de Castro, J.M., Weber, G.W., Zaidner, Y., Hershkovitz, I., 2021. Response to comment on "A Middle Pleistocene *Homo* from Nesher Ramla, Israel". Science 374, eabl5789.
Mellars, P., 1999. The Neanderthal problem continued. Curr. Anthropol. 40, 341–364.
Meyer, M., Arsuaga, J.-L., de Filippo, C., Nagel, S., Aximu-Petri, A., Nickel, B., Martínez, I., Gracia, A., Bermúdez de Castro, J.M., Carbonell, E., Viola, B., Kelso, J., Prüfer, K., Pääbo, S., 2016. Nuclear DNA sequences from the Middle Pleistocene Sima de los Huesos hominins. Nature 531, 504–507.
Mounier, A., Marchal, F., Condemi, S., 2009. Is *Homo heidelbergensis* a distinct species? New insight on the Mauer mandible. J. Hum. Evol. 56, 219–246.
Muttoni, G., Scardia, G., Kent, D.V., Swisher, C.C., Manzi, G., 2009. Pleistocene magnetochronology of early hominin sites at Ceprano and Fontana Ranuccio, Italy. Earth Planet Sci. Lett. 286, 255–268.
Nicholson, E., Harvati, K., 2006. Quantitative analysis of human mandibular shape using three-dimensional geometric morphometrics. Am. J. Phys. Anthropol. 131, 368–383.
Ossenberg, N.S., 1974. The mylohyoid bridge: An anomalous derivative of Meckel's Cartilage. J. Dent. Res. 53, 77–82.
Petr, M., Hajdinjak, M., Fu, Q., Essel, E., Rougier, H., Crevecoeur, I., Semal, P., Golovanova, L.V., Doronichev, V.B., Lalueza-Fox, C., de la Rasilla, M., Rosas, A., Shunkov, M.V., Kozlikin, M.B., Derevianko, A.P., Vernot, B., Meyer, M., Kelso, J., 2020. The evolutionary history of Neanderthal and Denisovan Y chromosomes. Science 369, 1653–1656.
Pirson, S., Toussaint, M., Bonjean, D., Di Modica, K., 2018. Spy and Scladina caves: A Neandertal's story. In: Demoulin, A. (Ed.), Landscapes and Landforms of

Belgium and Luxembourg, World Geomorphological Landscapes. Springer International Publishing, Cham, pp. 357–383.
Posth, C., Wißing, C., Kitagawa, K., Pagani, L., van Holstein, L., Racimo, F., Wehrberger, K., Conard, N.J., Kind, C.J., Bocherens, H., Krause, J., 2017. Deeply divergent archaic mitochondrial genome provides lower time boundary for African gene flow into Neanderthals. Nat. Commun. 8, 16046.
Prüfer, K., Racimo, F., Patterson, N., Jay, F., Sankararaman, S., Sawyer, S., Heinze, A., Renaud, G., Sudmant, P.H., de Filippo, C., Li, H., Mallick, S., Dannemann, M., Fu, Q., Kircher, M., Kuhlwilm, M., Lachmann, M., Meyer, M., Ongyerth, M., Siebauer, M., Theunert, C., Tandon, A., Moorjani, P., Pickrell, J., Mullikin, J.C., Vohr, S.H., Green, R.E., Hellmann, I., Johnson, P.L.F., Blanche, H., Cann, H., Kitzman, J.O., Shendure, J., Eichler, E.E., Lein, E.S., Bakken, T.E., Golovanova, L.V., Doronichev, V.B., Shunkov, M.V., Derevianko, A.P., Viola, B., Slatkin, M., Reich, D., Kelso, J., Pääbo, S., 2014. The complete genome sequence of a Neanderthal from the Altai Mountains. Nature 505, 43–49.
Prüfer, K., Posth, C., Yu, H., Stoessel, A., Spyrou, M.A., Deviese, T., Mattonai, M., Ribechini, E., Higham, T., Velemínský, P., 2021. A genome sequence from a modern human skull over 45,000 years old from Zlatý kůň in Czechia. Nat. Ecol. Evol. 5, 820–825.
Puech, P.-F., Puech, S., 1993. L'usure des dents de Banyoles. In: La Mandíbula de Banyoles En El Context Eels Fòssils Humans Del Pleistocè. Centre d'investigacions arqueològiques sèrie monogràfica, Girona, pp. 105–115.
Quam, R.M., Smith, F.H., 2002. A reassessment of the Tabun C2 mandible. In: Akazawa, T., Aoki, K., Bar-Yosef, O. (Eds.), Neandertals and Modern Humans in Western Asia. Kluwer Academic Publishers, Boston, pp. 405–421.
Quam, R.M., Arsuaga, J.-L., Bermúdez de Castro, J.-M., Díez, C.J., Lorenzo, C., Carretero, M., García, N., Ortega, A.I., 2001. Human remains from Valdegoba Cave (Huérmeces, Burgos, Spain). J. Hum. Evol. 41, 385–435.
Quam, R.M., Martínez, I., Arsuaga, J.-L., 2011. New observations on the human fossils from Petit-Puymoyen (Charente). PaleoAnthropology 95–105.
R Core Team, 2022. R: A language and environment for statistical computing. R Foundation for Statistical Computing, Vienna, Austria. https://www.R-project.org/.
Rak, Y., 1986. The Neanderthal: A new look at an old face. J. Hum. Evol. 15, 151–164.
Rak, Y., Kimbel, W.H., Hovers, E., 1994. A Neandertal infant from Amud Cave, Israel. J. Hum. Evol. 26, 313–324.
Rak, Y., Ginzburg, A., Geffen, E., 2002. Does *Homo neanderthalensis* play a role in modern human ancestry? The mandibular evidence. Am. J. Phys. Anthropol. 119, 199–204.
Rink, W.J., Schwarcz, H.P., Lee, H.K., Rees-Jones, J., Rabinovich, R., Hovers, E., 2001. Electron spin resonance (ESR) and thermal ionization mass spectrometric (TIMS)230Th/234U dating of teeth in Middle Paleolithic layers at Amud Cave, Israel. Geoarchaeology 16, 701–717.
Roksandic, M., Mihailović, D., Mercier, N., Dimitrijević, V., Morley, M.W., Rakočević, Z., Mihailović, B., Guibert, P., Babb, J., 2011. A human mandible (BH-1) from the Pleistocene deposits of Mala Balanica cave (Sićevo Gorge, Niš, Serbia). J. Hum. Evol. 61, 186–196.
Rosas, A., 1993. Las mandibulas humanas de Atapuerca: Un planteamiento desde al biologia del desarrollo. In: Maroto, J. (Ed.), La Mandíbula de Banyoles En El Context Eels Fòssils Humans Del Pleistocè. Centre d'investigacions arqueològiques sèrie monogràfica, Girona, pp. 189–194.
Rosas, A., 2001. Occurrence of Neanderthal features in mandibles from the Atapuerca-SH site. Am. J. Phys. Anthropol. 114, 74–91.
Rosas, A., Bastir, M., 2002. Thin-plate spline analysis of allometry and sexual dimorphism in the human craniofacial complex. Am. J. Phys. Anthropol. 117, 236–245.
Rosas, A., Bastir, M., 2004. Geometric morphometric analysis of allometric variation in the mandibular morphology of the hominids of Atapuerca, Sima de los Huesos site. Anat. Rec. 278A, 551–560.
Rosas, A., Bermúdez De Castro, J.M., 1998. On the taxonomic affinities of the Dmanisi mandible (Georgia). Am. J. Phys. Anthropol. 107, 145–162.
Rosas, A., Bastir, M., Alarcón, J.A., 2019. Tempo and mode in the Neandertal evolutionary lineage: A structuralist approach to mandible variation. Quat. Sci. Rev. 217, 62–75.
Roth, H., 1982. Les arcades alveolaire et dentaire de l'homme de Tautavel, I. In: L'*Homo erectus* et La Place de l'homme de Tautavel Parmi Les Hominidés Fossiles. Congrès International de Paléontologie Humaine, Paris, pp. 222–248.
Roth, H., Simon, C., Maroto, J., 1993. Situation de l'homme de Banyoles: Anteneandertalien ou Neandertalien? Une evaluation metrique de l'arcade dentaire. In: La Mandíbula de Banyoles En El Context Dels Fòssils Humans Del Pleistocè. Centre d'investigacions arqueològiques sèrie monogràfica, Girona, pp. 165–178.
RStudio Team, 2022. RStudio: Integrated development for R. RStudio, Inc., Boston, MA (Computer Software v02.1+461). http://www.rstudio.com/.
Sánchez-Lopez, F., 1993. Presencia de caracteres autapomórficos neandertalenses en la mandíbula de Banyoles. In: Maroto, J. (Ed.), La Mandíbula de Banyoles En El Context Dels Fòssils Humans Del Pleistocè. Centre d'investigacions arqueològiques sèrie monogràfica, Girona, pp. 79–188.
Sánchez-Quinto, F., Botigué, L.R., Civit, S., Arenas, C., Ávila-Arcos, M.C., Bustamante, C.D., Comas, D., Lalueza-Fox, C., 2012. North African populations carry the signature of admixture with Neandertals. PLoS One 7, e47765.
Sankararaman, S., Patterson, N., Li, H., Pääbo, S., Reich, D., 2012. The date of interbreeding between Neandertals and modern humans. PLoS Genet. 8, e1002947.
Schmerling, P.C., 1833. Recherches sur les ossemens fossiles découverts dans les cavernes de la province de Liège, Recherches sur les ossemens fossiles découverts dans les cavernes de la province de Liège, 1. Guez P.J. Collardin, Liége.
Schwarcz, H.P., Buhay, W.M., Grün, R., Valladas, H., Tchernov, E., Bar-Yosef, O., Vandermeersch, B., 1989. ESR dating of the Neanderthal site, Kebara Cave, Israel. J. Archaeol. Sci. 16, 653–659.
Schwartz, J.H., Tattersall, I., 2000. The human chin revisited: What is it and who has it? J. Hum. Evol. 38, 367–409.
Sergi, S., 1917. La Mandibola di Bañolas. Rev. Antropol. 22, 311–315.
Shearer, B.M., Cooke, S.B., Halenar, L.B., Reber, S.L., Plummer, J.E., Delson, E., Tallman, M., 2017. Evaluating causes of error in landmark-based data collection using scanners. PLoS One 12, e0187452.
Slimak, L., Zanolli, C., Higham, T., Frouin, M., Schwenninger, J.-L., Arnold, L.J., Demuro, M., Douka, K., Mercier, N., Guérin, G., Valladas, H., Yvorra, P., Giraud, Y., Seguin-Orlando, A., Orlando, L., Lewis, J.E., Muth, X., Camus, H., Vandevelde, S., Buckley, M., Mallol, C., Stringer, C., Metz, L., 2022. Modern human incursion into Neanderthal territories 54,000 years ago at Mandrin, France. Sci. Adv. 8, eabj9496.
Smith, F.H., 1978. Evolutionary significance of the mandibular foramen area in Neandertals. Am. J. Phys. Anthropol. 48, 523–531.
Smith, F.H., 2013. The fate of the Neandertals. J. Anthropol. Res. 69, 167–200.
Smith, F.H., Ahern, J.C.M., Janković, I., Karavanić, I., 2017. The Assimilation Model of modern human origins in light of current genetic and genomic knowledge. Quat. Int. 450, 126–136.
Solé Sabarís, L., 1957. Generalités, Empordá, Region volcanique d'Olot, Cerdagne, Andorre, vallées du Segre et de l'Aragon (II Journée. Gérone, Banyoles, Olot, Ripoll et Núria). In: INQUA, Congrès International. Livret guide de l'excursion N1. Pyrénées, Madrid-Barcelona, V, pp. 34–43.
Spencer, M.A., Demes, B., 1993. Biomechanical analysis of masticatory system configuration in Neandertals and Inuits. Am. J. Phys. Anthropol. 91, 1–20.
Stefan, V.H., Trinkaus, E., 1998. La Quina 9 and Neandertal mandibular variability. Bull. Mem. Soc. Anthropol. Paris 10, 293–324.
Stringer, C.B., Hublin, J.J., Vandermeersch, B., 1984. The origin of anatomically modern humans in western Europe. In: Smith, F.H., Spencer, F. (Eds.), The Origins of Modern Humans: A World Survey of the Fossil Evidence. Alan R. Liss, New York, pp. 51–135.
Suganuma, Y., Okada, M., Head, M.J., Kameo, K., Haneda, Y., Hayashi, H., Irizuki, T., Itaki, T., Izumi, K., Kubota, Y., 2021. Formal ratification of the global boundary stratotype section and point (GSSP) for the Chibanian stage and Middle Pleistocene subseries of the Quaternary system: the Chiba section, Japan. Episodes J. Int. Geosci. 44, 317–347.
Tattersall, I., 2011. Before the Neanderthals: Hominid evolution in middle Pleistocene Europe. In: Condemi, S., Weniger, G.C. (Eds.), Continuity and Discontinuity in the Peopling of Europe. Springer Netherlands, Dordrecht, pp. 47–53.
Tattersall, I., Schwartz, J.H., 1999. Hominids and hybrids: The place of Neanderthals in human evolution. Proc. Natl. Acad. Sci. USA 96, 7117–7119.
Trinkaus, E., 1987. The Neandertal face: Evolutionary and functional perspectives on a recent hominid face. J. Hum. Evol. 16, 429–443.
Trinkaus, E., 2006. Modern human versus Neandertal evolutionary distinctiveness. Curr. Anthropol. 47, 597–620.
Trinkaus, E., Rougier, H., 2013. The human mandible from the Peştera cu Oase, Oase 1. In: Trinkaus, E., Constantin, S., Zilhão, J. (Eds.), Life and Death at the Peştera Cu Oase: A Setting for Modern Human Emergence in Europe. Oxford University Press, Oxford, pp. 234–256.
Trinkaus, E., Shipman, P., 1993. The Neanderthals: Changing the Image of Mankind, 1st. Knopf, New York.
Trinkaus, E., Moldovan, O., Milota, Stefan, Bîlgăr, A., Sarcina, L., Athreya, S., Bailey, S.E., Rodrigo, R., Mircea, G., Higham, T., Ramsey, C.B., van der Plicht, J., 2003. An early modern human from the Peştera cu Oase, Romania. Proc. Natl. Acad. Sci. USA 100, 11231–11236.
Vandermeersch, B., Trinkaus, E., 1995. The postcranial remains of the Régourdou 1 Neandertal: The shoulder and arm remains. J. Hum. Evol. 28, 439–476.
Van Andel, T.H., Davies, W., Weninger, B., 2003. The human presence in Europe during the Last Glacial Period I: Human migrations and the changing climate. In: Van Andel, T.H., Davies, W. (Eds.), Neanderthals and Modern Humans in the European Landscape during the Last Glaciation: Archaeological Results of the Stage 3 Project. McDonald Institute for Archaeological Research, Cambridge, pp. 31–56.
Verna, C., Détroit, F., Kupczik, K., Arnaud, J., Balzeau, A., Grimaud-Hervé, D., Bertrand, S., Riou, B., Moncel, M.-H., 2020. The Middle Pleistocene hominin mandible from Payre (Ardèche, France). J. Hum. Evol. 144, 102775.
Vialet, A., Modesto-Mata, M., Martinón-Torres, M., Martínez de Pinillos, M., Bermúdez de Castro, J.-M., 2018. A reassessment of the Montmaurin-La Niche mandible (Haute Garonne, France) in the context of European Pleistocene human evolution. PLoS One 13, e0189714.
Vlcek, E., 1993. Fossile menschenfunde von Weimar-Ehringsdorf. Konrad Theiss, Verlag, Stuttgart.
Wall, J.D., Yang, M.A., Jay, F., Kim, S.K., Durand, E.Y., Stevison, L.S., Gignoux, C., Woerner, A., Hammer, M.F., Slatkin, M., 2013. Higher levels of Neanderthal ancestry in East Asians than in Europeans. Genetics 194, 199–209.
Weber, G.W., Bookstein, F.L., 2011. Virtual Anthropology: A Guide to a New Interdisciplinary Field, first ed. Springer-Verlag, Vienna.
Weidenreich, F., 1936. The mandibles of *Sinanthropus pekinensis*: A comparative study. Paleontol. Sin., D 7, 1–162.
Wickham, H., 2009. Ggplot2: Elegant graphics for data analysis (Use R!). Springer, New York.
Wood, B., 1991. Koobi Fora research project: Researches into geology, palaeontology, and human origins. In: Hominid Cranial Remains, vol. 4. Clarendon Press, Oxford.
Yokoyama, Y., Shen, G., Nguyen, H., Falguères, C., 1987. Datation du travertin de Banyoles à Gérone, Espagne. Cypsela 155–160.